Musculoskeletal Ultrasound

Author(s) Beggs, Ian

Imprint Lippincott Williams & Wilkins, 2014

ISBN 9781451144987, 1451144989

Permalink https://books-scholarsportal-info.myaccess.library.utoronto.ca/en/xml/chapter?id=/ebooks/ebooks1/lww/2014-07-29/1/01762492&chapterId=B01762492-C3

Chapter 3
Shoulder
Ian Beggs

INTRODUCTION

Ultrasound has become increasingly important in the assessment of the shoulder in recent years. It is as accurate as magnetic resonance imaging (MRI) in diagnosing rotator cuff tears[1] and is also cheap and quick. Patients prefer ultrasound to MRI.[2] The relative ease of access makes ultrasound ideal for a "one-stop shop" approach.[3] Ultrasoundguided interventions are widely used. The objection that ultrasound is operator-dependent applies to other imaging techniques, clinical assessment, and surgical interventions.

ANATOMY AND EXAMINATION TECHNIQUE

The anatomy and examination technique of the shoulder is well illustrated on the website of the European Society of Musculoskeletal Radiology.[4]

The tendons of the four muscles that contribute to the rotator cuff coalesce to insert on the greater and lesser tuberosities of the humerus (Fig. 3.1). Subscapularis originates from the anterior surface of the scapular blade and inserts on the lesser tuberosity. Supraspinatus originates from the suprascapular fossa and infraspinatus and teres minor from the dorsal surface of the scapula inferior to its spine. They insert in sequence from anterior to posterior on the greater tuberosity: supraspinatus on the superior facet and infraspinatus on the middle facet, although the footprint of the infraspinatus tendon is larger than that of supraspinatus and occupies much more of the tuberosity than previously thought. Teres minor inserts posterior to infraspinatus. Overlapping tendon fibers diffuse the load across the cuff rather than being concentrated in a single tendon.[5,6] The subacromial/subdeltoid bursa is interposed between the rotator cuff tendons and the coracoacromial arch, which comprises the coracoid, acromion, coracoacromial ligament (CAL), and acromioclavicular joint (ACJ) (Fig. 3.2).

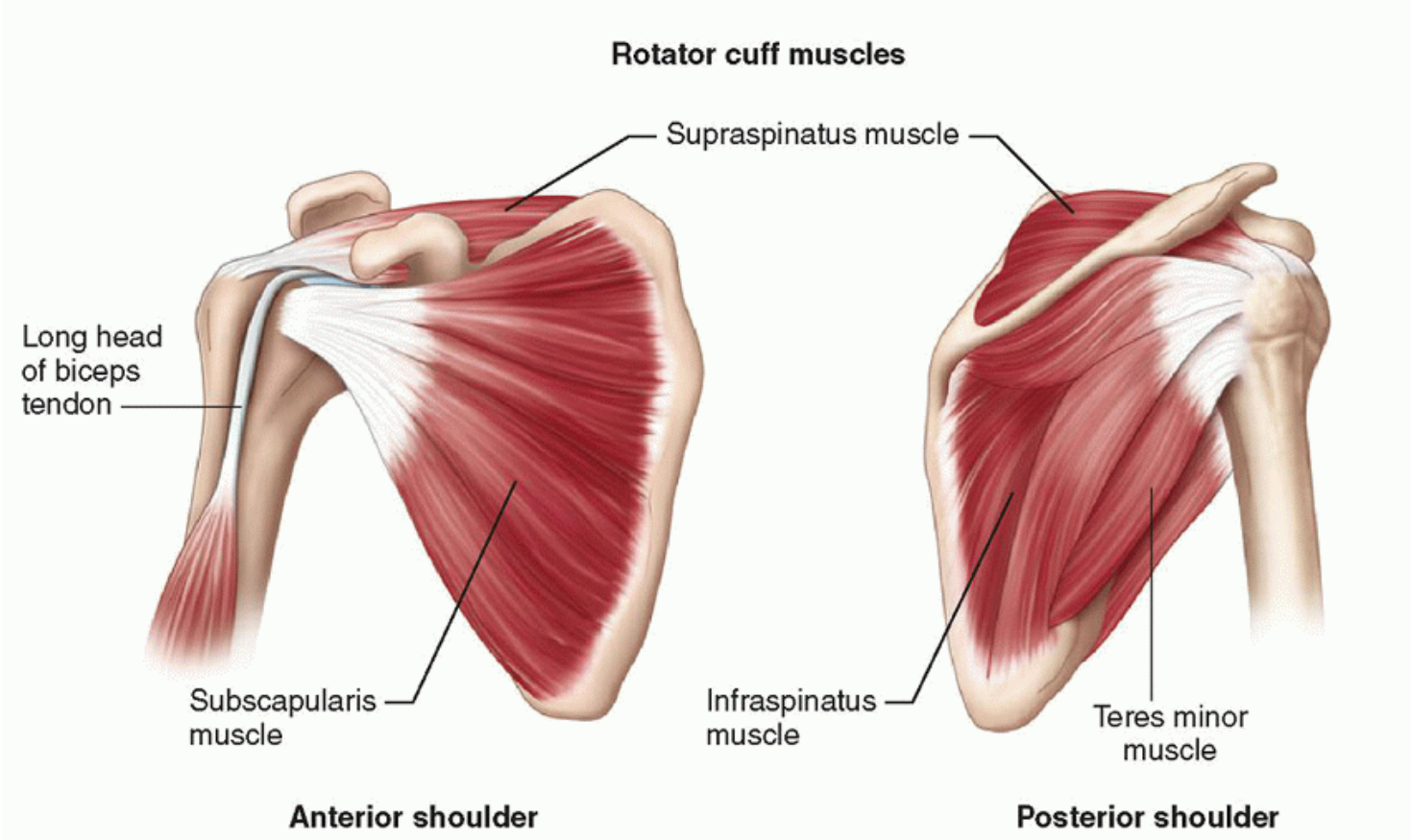

Figure 3.1. Subscapularis originates from the anterior surface of the scapular blade. Supraspinatus originates from the supraspinatus fossa on the posterior aspect of the scapula. Infraspinatus and teres minor originate below the scapular spine. The long head of biceps tendon lies between subscapularis and supraspinatus and is an important ultrasound landmark.

The long head of biceps (LHB) tendon is not part of the rotator cuff, but it is an important anatomical landmark. It originates from the superior glenoid labrum at the supraglenoid tubercle and runs through the joint,

separating subscapularis from the other rotator cuff tendons at the rotator interval (Fig. 3.1), then enters the bicipital groove and runs distally to its myotendinous junction in the mid-arm.

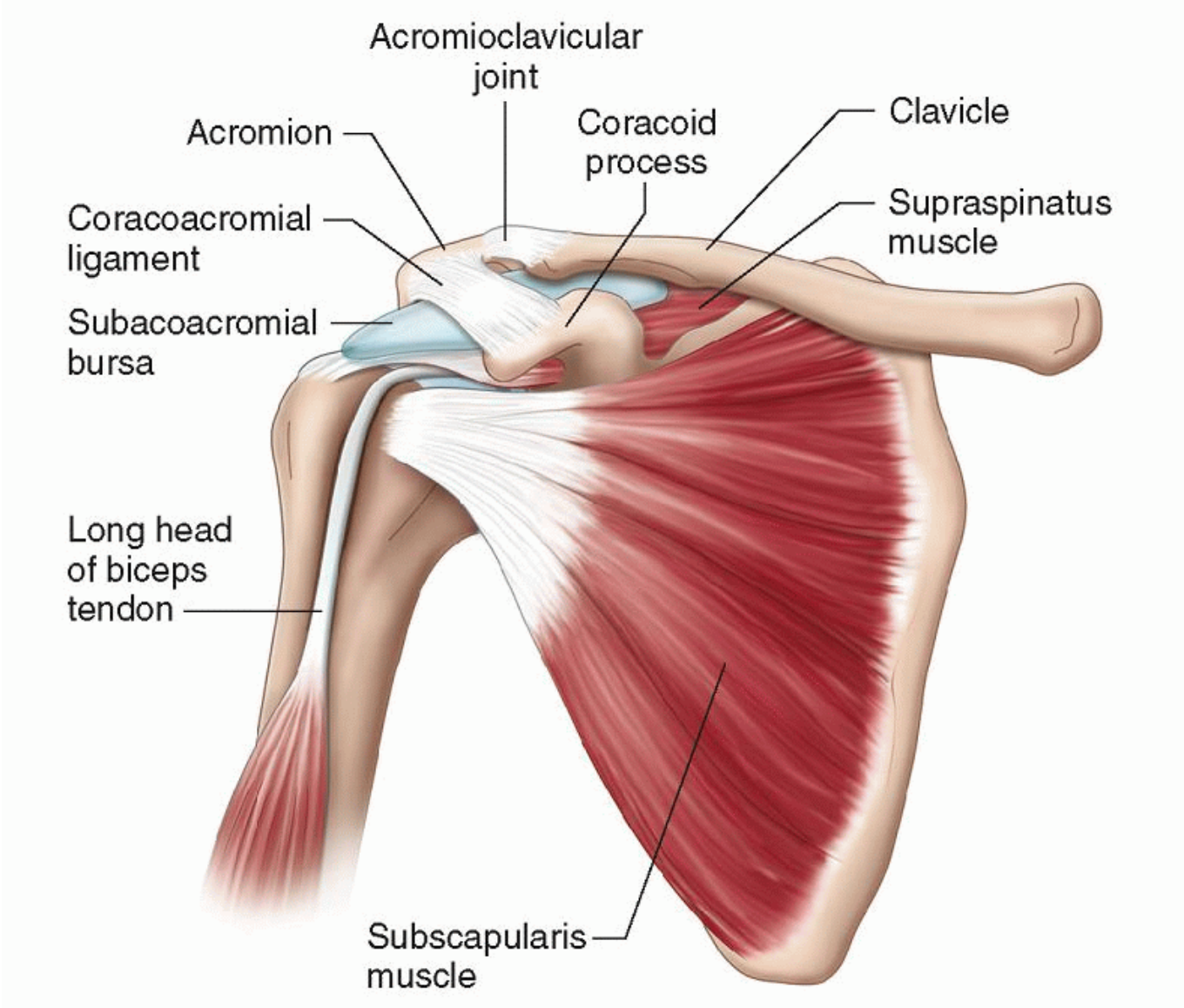

Figure 3.2. The subacromial bursa lies between the rotator cuff tendons and the coracoacromial arch.

Supraspinatus and infraspinatus are innervated by the suprascapular nerve, a branch of the brachial plexus that passes through the suprascapular notch to supply supraspinatus and then through the spinoglenoid notch to supply infraspinatus. Subscapularis is supplied by subscapular branches of the brachial plexus and teres minor by the axillary nerve.

The articular cortex of the humeral head is usually smooth, although small pits are common. The greater and lesser tuberosities are usually slightly flat and depressed relative to the articular cortex. Hyaline cartilage covers the articular cortex. Enthesis fibrocartilage covers the tuberosities. Both types of cartilage are anechoic on ultrasound and appear in continuity.

ULTRASOUND EXAMINATION: TECHNIQUE AND APPEARANCES

In contrast to most other joints where the examination is targeted at a particular part of the joint to address a specific problem, ultrasound of the shoulder is usually a “whole joint” examination and is performed in a routine sequence.[7,8]

The patient is seated on a swivel chair and the height adjusted so that the patient’s shoulder is at a comfortable level for the examiner who stands in front of or behind the patient. I prefer to stand behind the patient. I can look over the patient at the ultrasound screen, lean forward to adjust the controls, and, importantly, support my hand on the patient’s shoulder. Standing in front of the patient places more stress on the examiner’s own shoulder.

Figure 3.3. The LHB tendon is examined with the patient's elbow flexed at 90 degrees and the hand palm-up on the lap. Black line, long head of biceps tendon (LHB), black box, position of transducer for transverse scan of LHB.

The examination starts with the patient's elbow flexed at 90 degrees and the hand supine on the lap (Fig. 3.3). A transverse scan shows the biceps tendon as a round, well-defined, homogeneously echogenic structure in the bicipital groove (Fig. 3.4). A thin echogenic transverse "ligament," probably actually fibers of the subscapularis tendon that continue from the lesser tuberosity to the greater tuberosity, covers the tendon at the entrance to the groove.

If the transducer is positioned slightly proximally, the biceps sling may be identified (Fig. 3.5). Moving the elbow posteriorly and rotating the transducer with the medial end slightly inferiorly may help. The sling is thought to be a more important stabiliser than the

transverse ligament. It is echogenic and has a horizontal U-shape with the base lying medially. The superior limb of the sling is the coracohumeral ligament (CHL), which merges with the anterior fibers of the supraspinatus tendon and also inserts on the greater tuberosity. The inferior limb is the superior glenohumeral ligament, which runs to the lesser tuberosity with some fibers of the CHL.[9,10]

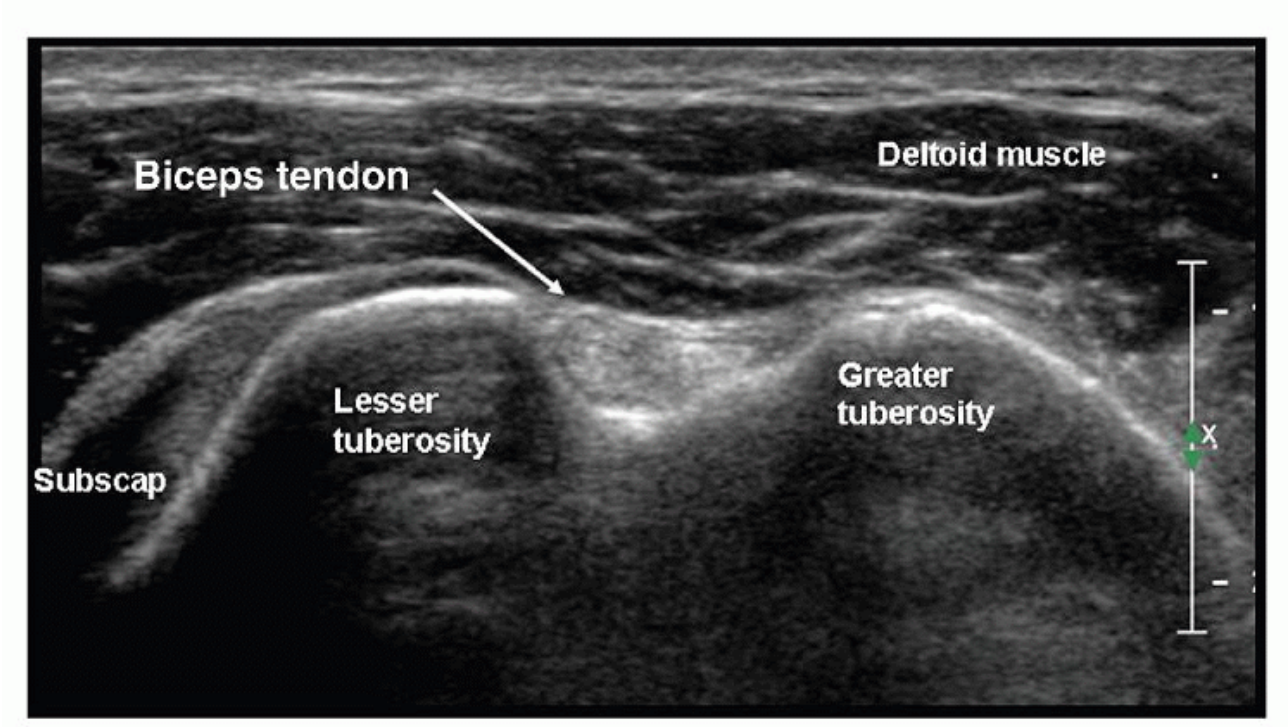

Figure 3.4. Biceps lies in the bicipital groove and appears round and echogenic on short-axis scans.

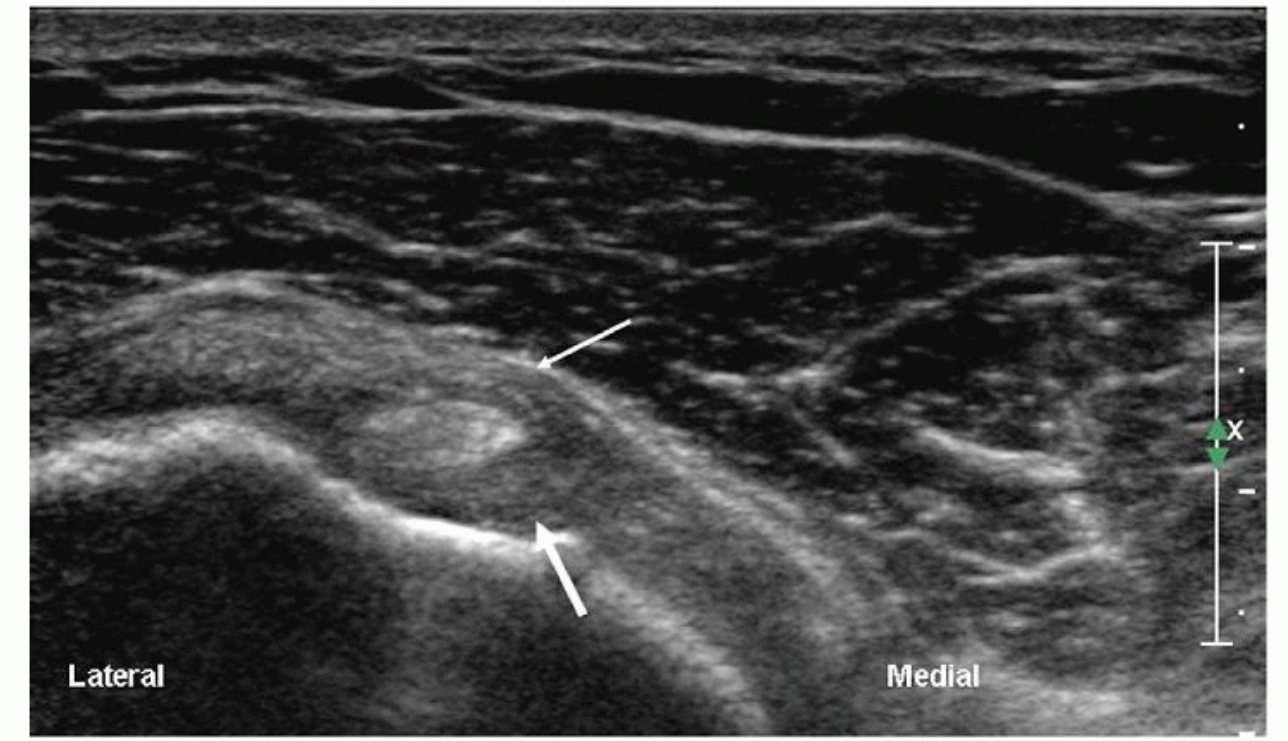

Figure 3.5. Transverse scan of LHB just proximal to bicipital groove. The tendon is stabilised by the biceps sling: the coracohumeral ligament (thin arrow) and the superior glenohumeral ligament (thick arrow).

The full length of the extra-articular biceps tendon is easily examined in transverse images by an “elevator” technique, running the transducer proximally and distally between the bicipital groove and the musculotendinous junction of biceps, which lies level with the insertion of the pectoralis major tendon (Fig. 3.6), on the humeral shaft. The normal biceps tendon is well defined and homogeneously echogenic. Small amounts of fluid in the tendon sheath are normal. If the transducer is rotated 90 degrees biceps can be examined longitudinally (Fig. 3.7), but this is less useful than transverse scanning. On longitudinal scans the tendon appears cord-like and striated. Variable amounts of the intra-articular biceps can be seen, but ultrasound is not an appropriate examination for suspected proximal biceps lesions such as SLAP tears.

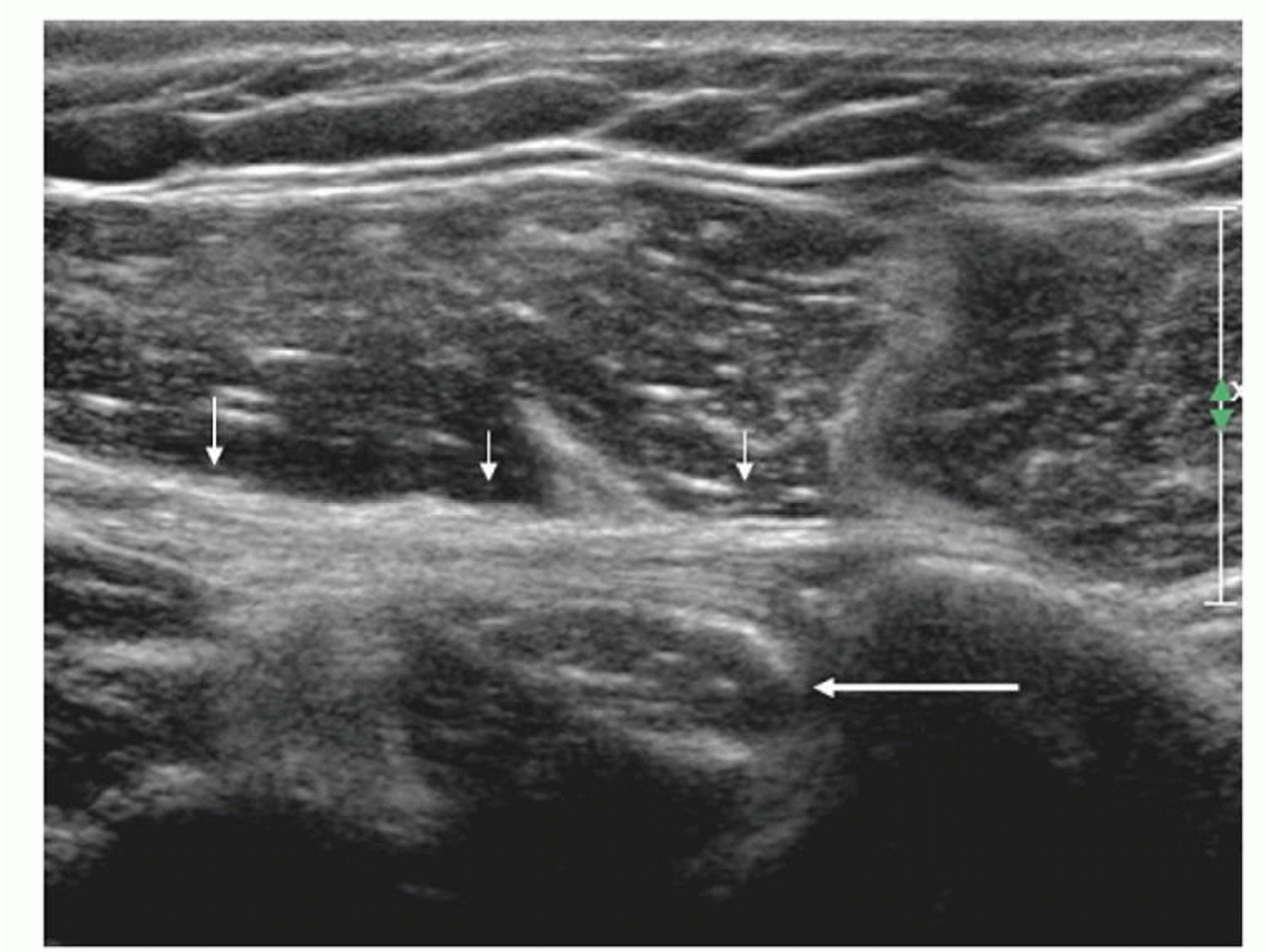

Figure 3.6. Transverse scan of arm at the level of pectoralis major tendon (short arrows), which inserts on the anterior humerus alongside the myotendinous junction of LHB (long arrow).

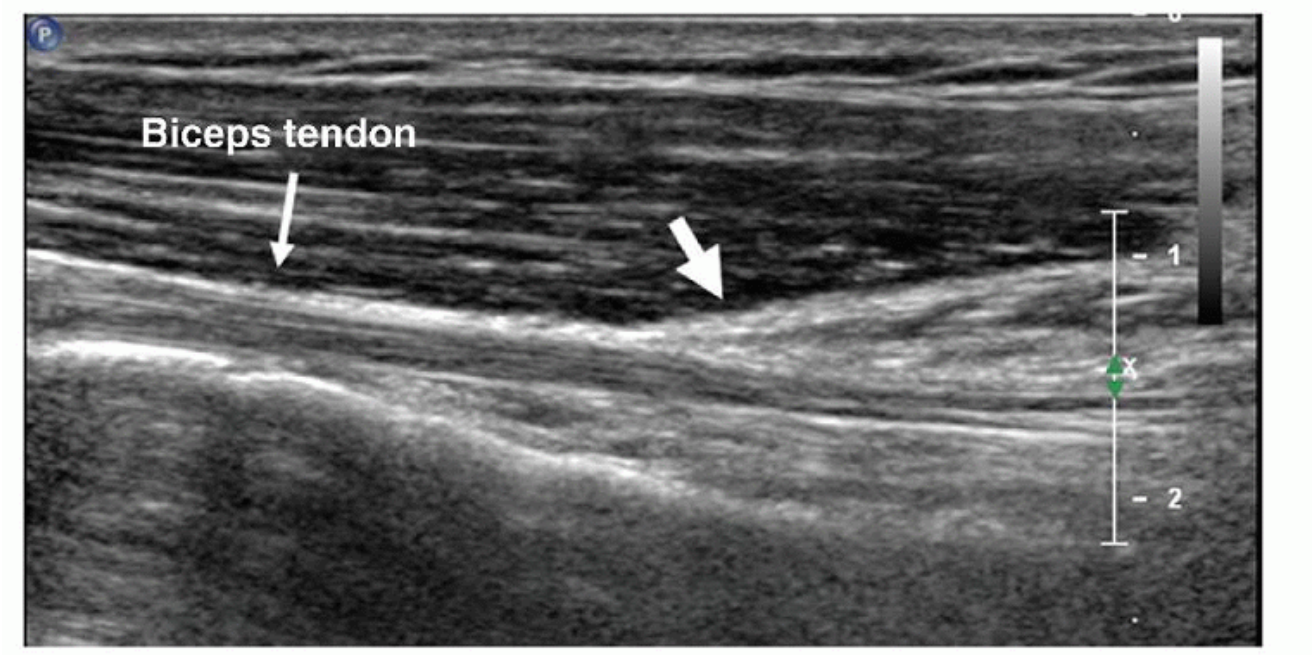

Figure 3.7. Longitudinal scan of LHB (thin arrow) and musculotendinous junction (thick arrow).
Next, to examine the subscapularis, the hand is externally rotated, still palm up with the elbow by the patient's side and flexed at 90 degrees (Fig. 3.8). A longaxis scan of subscapularis (Fig. 3.9), with the transducer lying transversely on the anterior shoulder, shows the hypoechoic muscle emerging from under the coracoid process and running as echogenic tendon to insert on the lesser tuberosity. The distal 1 cm or so of the tendon may appear hypoechoic owing to anisotropy if the transducer is not angled "round the corner" of the tuberosity. On transverse images the tendon is echogenic and has curved superior and inferior margins. Alternating

hypoechoic and echogenic areas at the myotendinous junction (Fig. 3.10) are due to muscle interspersed between multiple tendon slips.

Figure 3.8. Subscapularis is examined with the elbow flexed at 90 degrees and the hand externally rotated. Place the transducer (black box) transversely, just medial to biceps (black line) to obtain a long-axis scan of subscapularis. Rotate the transducer through 90 degrees for a short-axis scan.

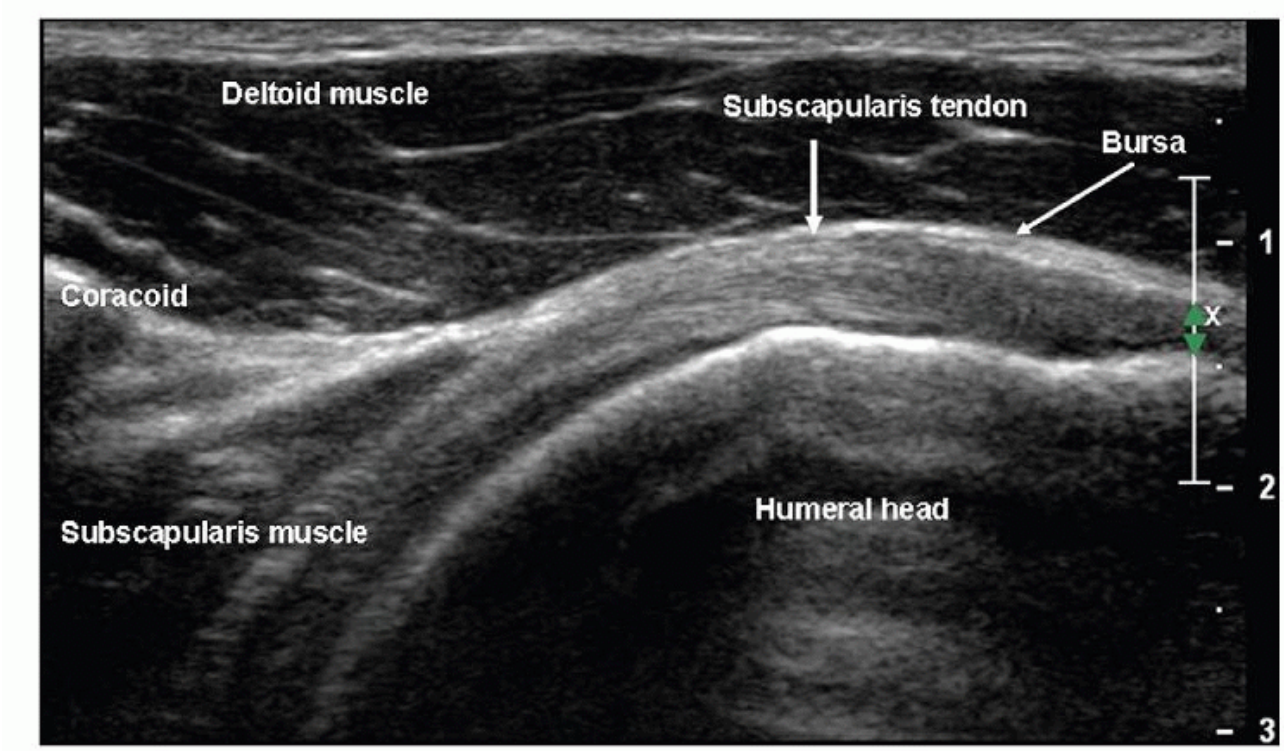

Figure 3.9. Long-axis scan of subscapularis. The muscle runs laterally under the coracoid process and is hypoechoic. The tendon is echogenic except distally where it appears hypoechoic due to anisotropy. The transducer must be angled or beam steering used to compensate.

Placing the transducer on the coracoid process and angling superiorly toward the acromion shows the CAL (Fig. 3.11). It is a thin, linear structure, small and oval on cross section.

Supraspinatus is examined with the shoulder internally rotated and extended to pull the tendon out from under the acromion. Three positions may be used. First, the hand is placed behind the lower back with palm facing backward (Fig. 3.12). This may be too painful in patients with severe tendinosis or impingement, and in young patients may result in too much internal rotation to show the anterior edge of supraspinatus. The alternatives, which achieve progressively less internal rotation, are to use the “hand-in-back-pocket” position with the hand prone on the lateral buttock, or simply to have the arm hanging by the side with the palm facing backward.

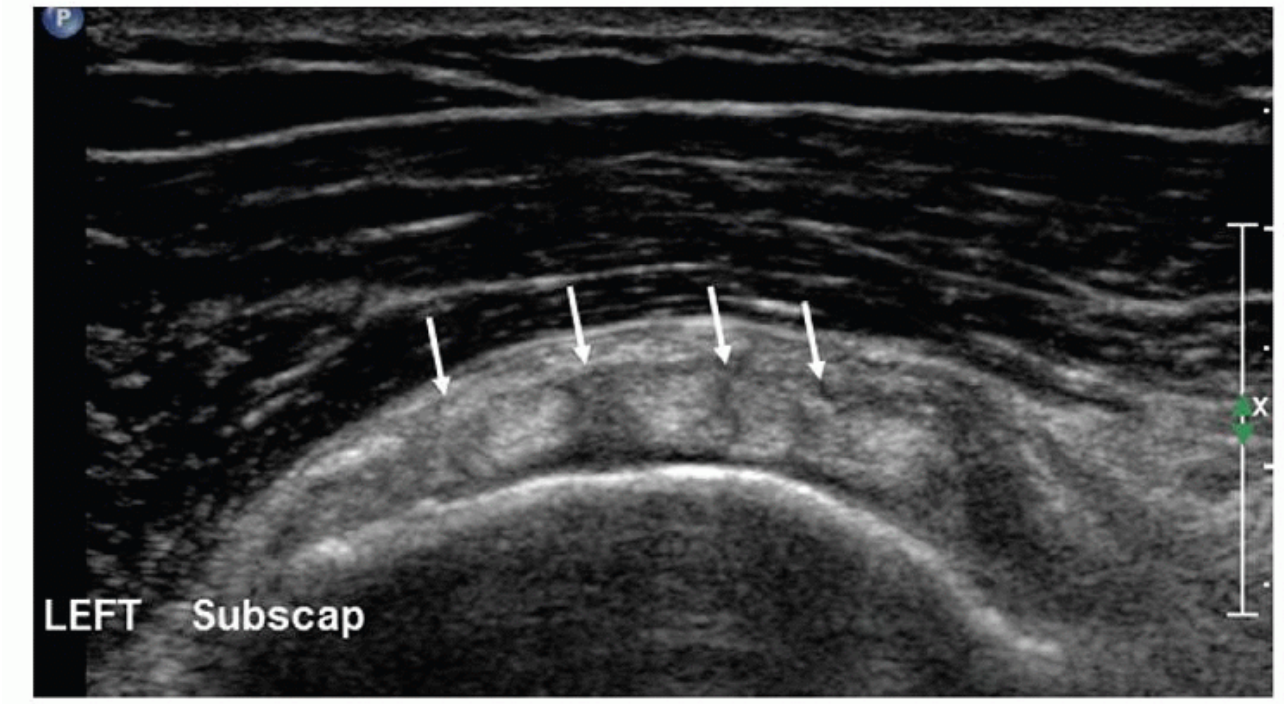

Figure 3.10. Short-axis scan of subscapularis at its musculotendinous junction. The slightly heterogeneous appearance is due to hypoechoic muscle (arrows) interposed between the echogenic tendon slips.

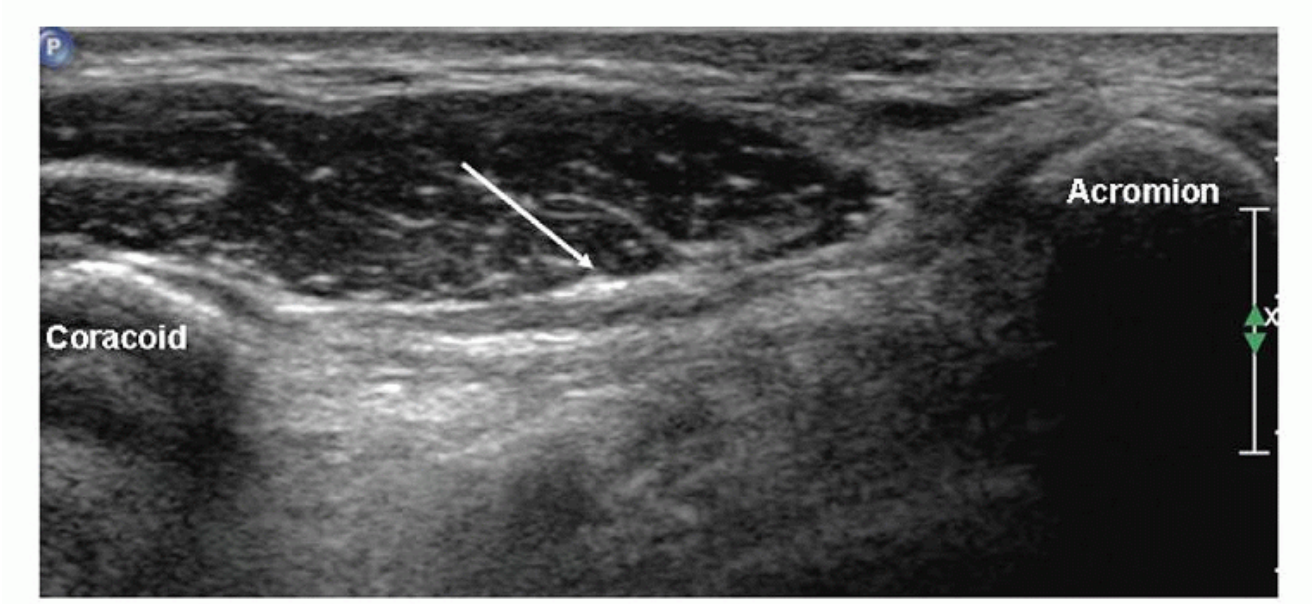

Figure 3.11. Coracoacromial ligament (arrow) is thin and broad and runs between the coracoid process and the acromion.

Tip:

If you can't see the rotator interval and anterior fibers of supraspinatus when the patient's hand is behind his or her back, the shoulder is too internally rotated. Try the "hand-in-back-pocket" or "hand-by-side" positions.

The transducer is placed parallel to the long axis or short axis of the tendon, equivalent to the coronal oblique and sagittal oblique views obtained with MRI. It is important to align the transducer to the axes of the tendon and not to body planes.

On long-axis views (Fig. 3.13) the tendon tapers smoothly toward its insertion on the greater tuberosity and has a convex superior surface. The thin, hypoechoic subacromial/subdeltoid bursa is superficial to supraspinatus and the other tendons of the cuff. Thin, parallel echogenic stripes of peribursal fat lie deep and superficial to the bursa. Fluid in the bursa can be an important clue to pathology, but may only be seen by scanning quite far distally, inferior to the tuberosities. Hypoechoic deltoid muscle overlies the bursa. There should therefore be three layers, deltoid, bursa/peribursal fat, and tendon, between the subcutaneous fat and the humeral head.

Tip:

Always identify three layers when examining supraspinatus: deltoid, bursa, and supraspinatus.

Supraspinatus is echogenic and has a uniformly striated appearance on long-axis images, but may appear hypoechoic if the angle of insonation is not 90 degrees. This occurs particularly distally where the tendon fibers swoop deeply to their insertion, and care must be taken to overcome the effect of anisotropy by altering the angle of the transducer and trying to "fill in" any hypoechoic areas.

Tip:

Try to "fill in" any hypoechoic areas in the rotator cuff by altering the angle of the transducer.

P. 30

Figure 3.12. Supraspinatus is examined with the arm extended, adducted, and internally rotated, with the hand behind the lower back and the palm facing backward to obtain long-axis (A) and short-axis (B) scans. Black boxes represent transducer positions. The entheseal fibrocartilage where the tendon inserts on the tuberosity is anechoic and appears virtually continuous with the hyaline cartilage on the articular cortex (Fig. 3.13), although a small bare area may be present at the junction between hyaline and entheseal cartilage. On short-axis images, supraspinatus has an echogenic speckled texture and is of uniform caliber, thinning progressively as it runs to its insertion. The anterior edge of supraspinatus normally overlaps the biceps tendon (Fig. 3.14).
The distal supraspinatus and infraspinatus tendons, which form the "rotator crescent," are relatively hypovascular[11] and are liable to injury. Occasionally, a small band of echogenic fibers, a few mm thick, runs transversely on the deep aspect of the tendon. This "rotator cable" appears to protect against tear propagation and reduces the functional disability caused by a rotator cuff tear.[12]

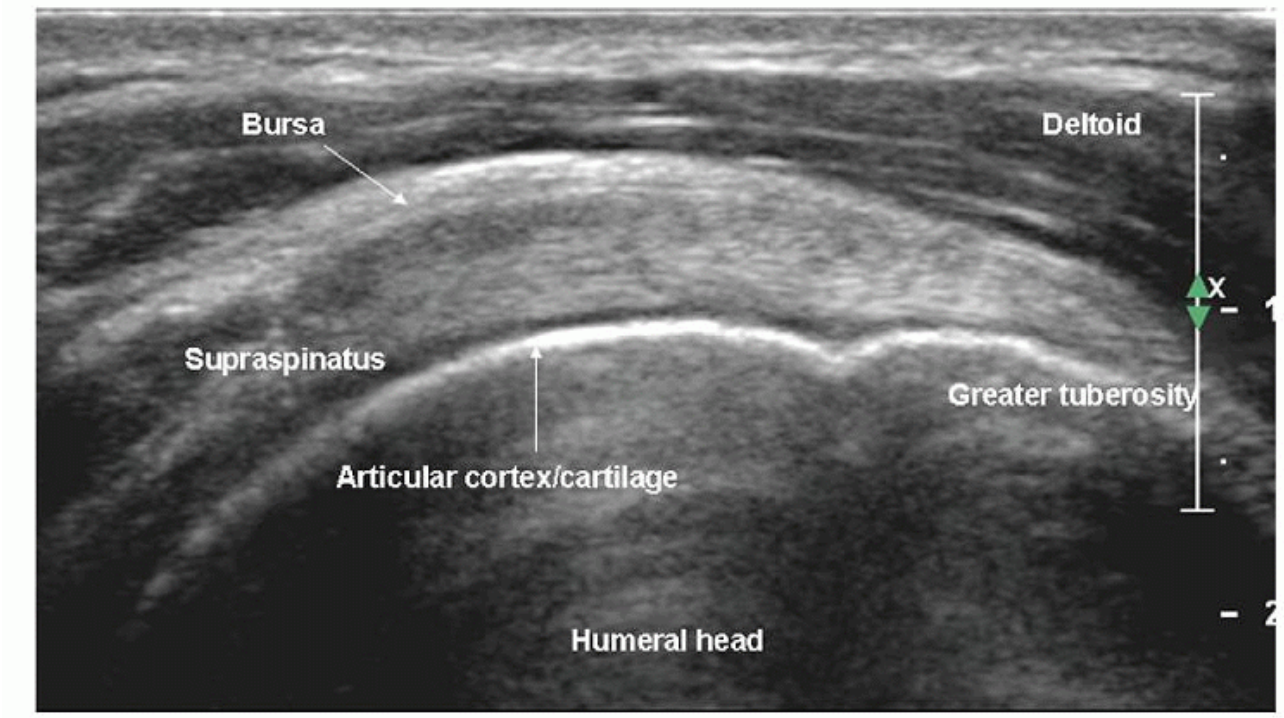

Figure 3.13. Longitudinal scan of supraspinatus. The tendon is homogeneously echogenic and tapers uniformly to its insertion on the greater tuberosity. There is a dip in the cortex between the tuberosity and the articular cortex. Anechoic cartilage covers the

humerus: hyaline cartilage over the articular cortex and fibrocartilage at the tuberosity. The thin hypoechoic bursa and the echogenic peribursal fat lie between the supraspinatus and deltoid.

Infraspinatus is examined with the elbow flexed, the forearm across the chest, the patient's hand palm down on the contralateral anterior chest wall, and the transducer placed transversely on the posterior aspect of the shoulder and angled slightly obliquely (Fig. 3.15). The hypoechoic infraspinatus muscle runs laterally and slopes gently superiorly. As it does so, the initially narrow intramuscular echogenic tendon widens to merge with the supraspinatus tendon and the hypoechoic muscle thins inversely. Deep to the infraspinatus (Fig. 3.16) is the posterior glenohumeral joint margin with the curved humeral head and the echogenic glenoid labrum. This is a good site to detect an effusion (Fig. 3.17), which elevates the capsule, or to inject into the joint. The spinoglenoid notch lies medially. A gangion due to internal derangement of the joint may extend to the notch and

compress the suprascapular nerve. The resulting infraspinatus weakness simulates a cuff tear.

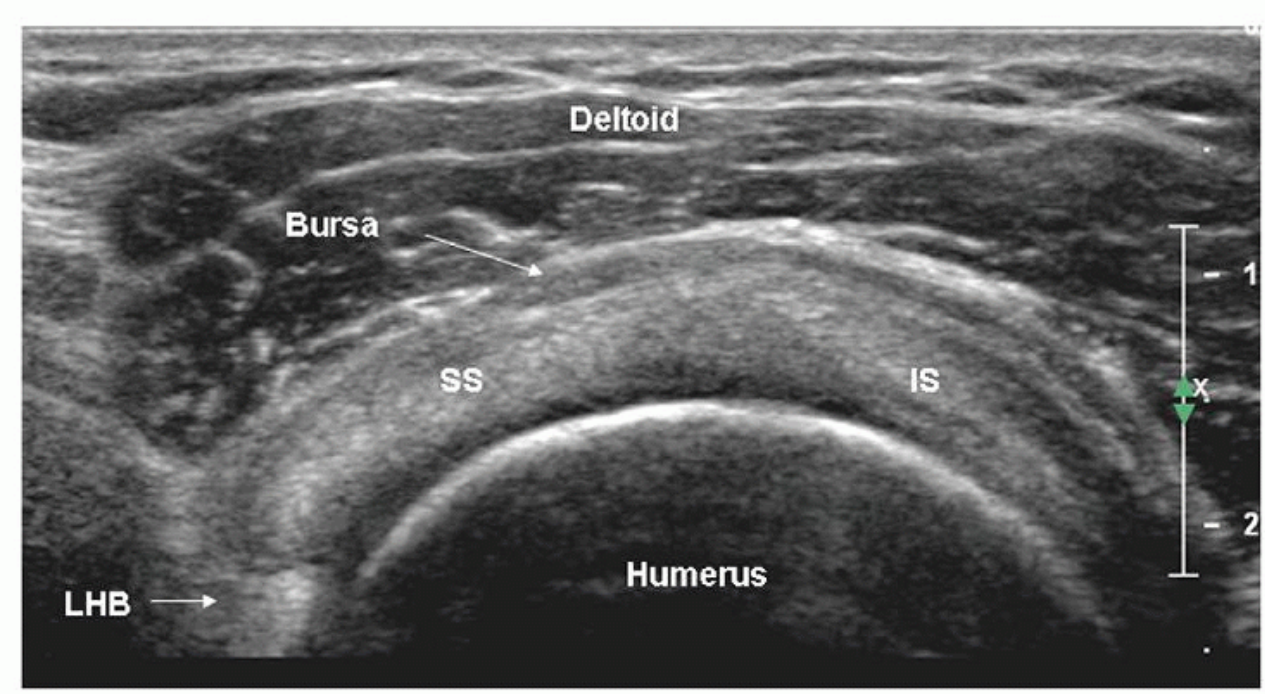

Figure 3.14. Short-axis scan of supraspinatus (SS) and infraspinatus (IS). The anterior edge of supraspinatus overlaps biceps (LHB). The bursa is thickened.

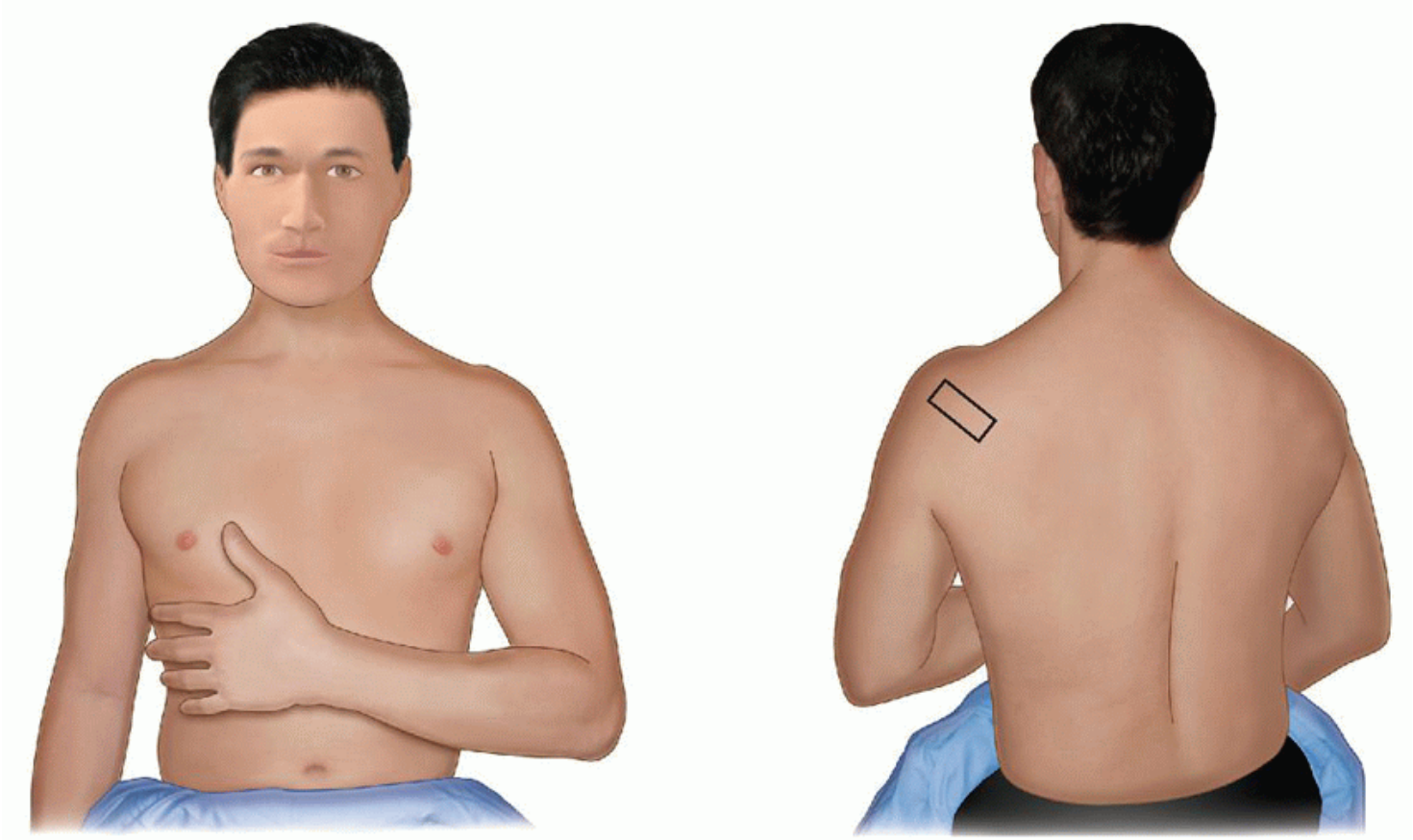

Figure 3.15. Infraspinatus is examined with the hand across the lower chest. The transducer (black box) is placed on the posterior glenohumeral joint line and angled obliquely upward to obtain long-axis views of the tendon.

Supraspinatus and infraspinatus form a continuous tendon sheet. Their junction may be recognised because of the slightly different orientations of the two tendons. It may be possible to identify the separate superior and middle facets of the greater tuberosity, the insertion sites of supraspinatus and infraspinatus, respectively. In practice, a distance of 1.5 cm behind the anterior edge of supraspinatus is said to mark the junction between the two tendons, although recent work suggests that infraspinatus may extend more anteriorly than this.[5] If supraspinatus is torn, biceps is a good proxy for its anterior edge.

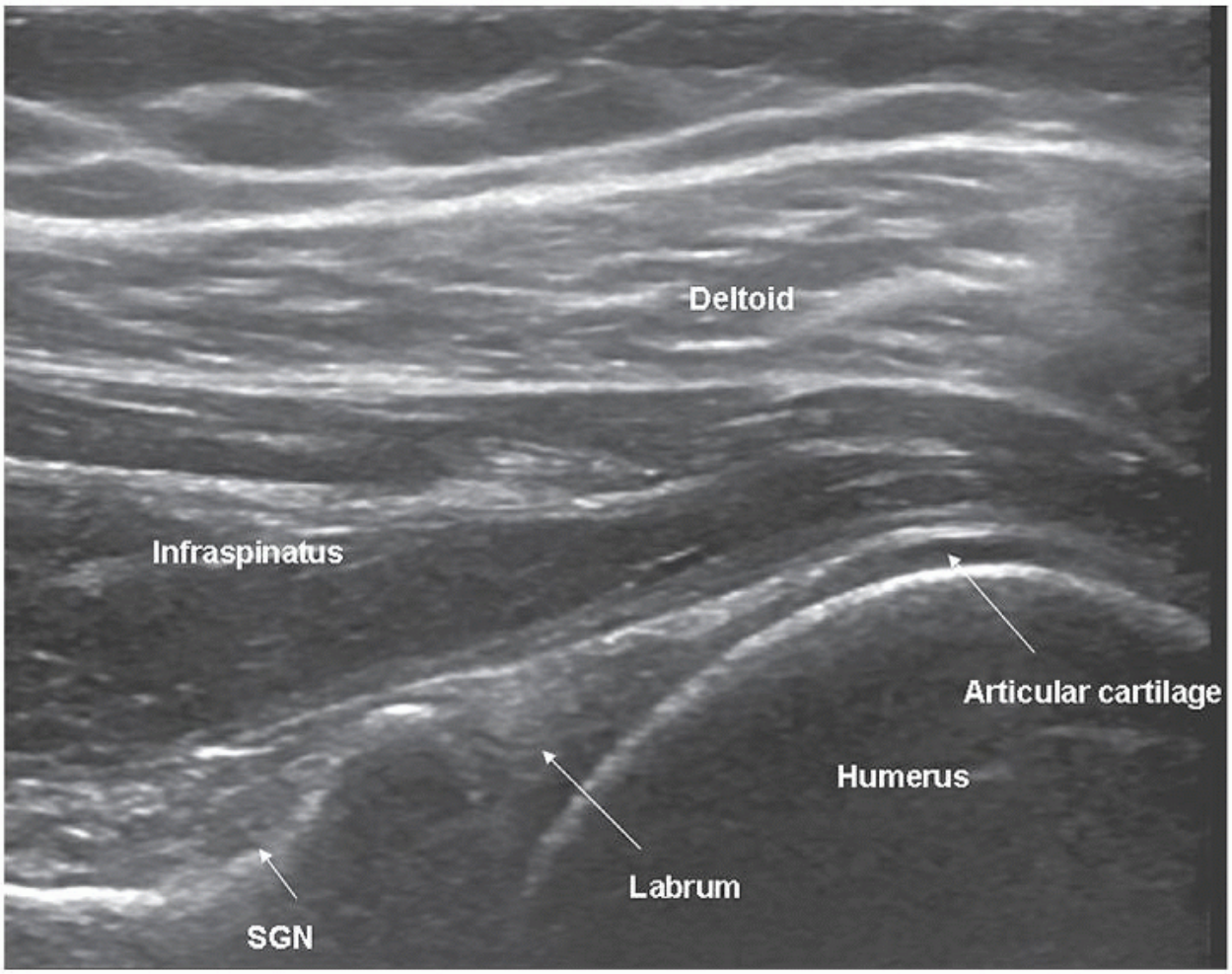

Figure 3.16. Transverse scan of the posterior joint line. The infraspinatus muscle sweeps anteriorly and superiorly toward the rotator cuff across the spinoglenoid notch (SGN), posterior labrum, and humeral head. This is a good position to detect small joint effusions and to inject into the glenohumeral joint.

This concludes the standard examination, although some examiners routinely include the ACJ or dynamic assessment of impingement. Teres minor is not usually examined. Muscle integrity should be assessed if a fullthickness rotator cuff tear is identified.

ROTATOR CUFF TENDINOSIS AND TEARS

Complete thickness tears; partial thickness tears; tendinosis; accuracy; asymptomatic tears; muscle atrophy and fatty infiltration; impingement.

Management of the painful shoulder is based on the concept of rotator cuff impingement. Neer[13] proposed that the interplay between the supraspinatus tendon and the coracoacromial arch, which includes the coracoid, anterior acromion, CAL, and ACJ, damages the tendon.

P. 32

The distal anterior supraspinatus tendon is especially vulnerable because it is avascular.[11],[14] Initially, reversible damage is followed by irreversible tendinosis and fibrosis and finally by rotator cuff tears.

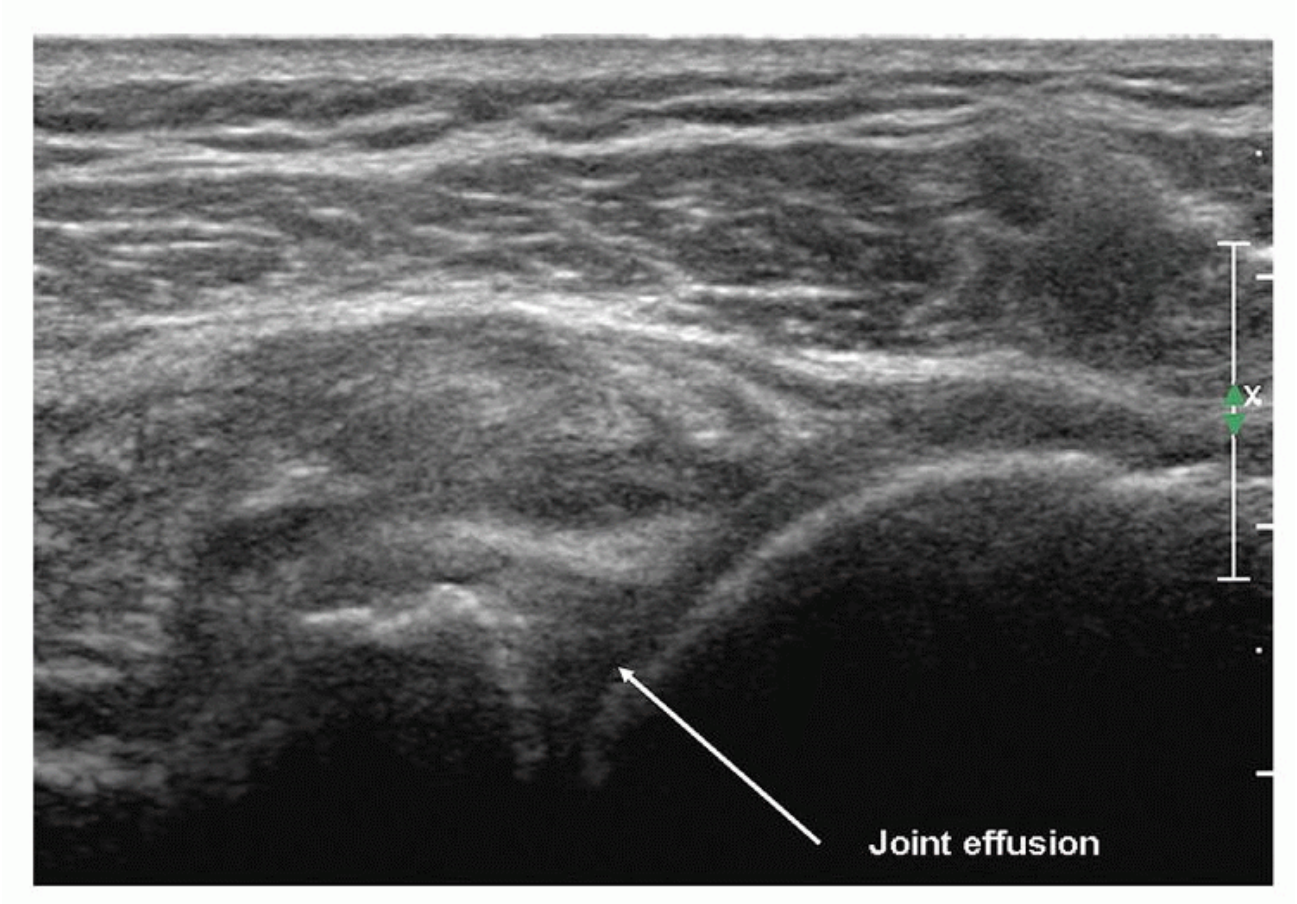

Figure 3.17. Small joint effusion (arrow) in a patient with a massive rotator cuff tear.

Clinical tests have only moderate sensitivity for rotator cuff tears[15,16] and are subject to considerable interobserver variability.[17] Experienced clinicians can accurately exclude rotator cuff tears, but depend on imaging to confirm if a tear is present.[18]

Full-thickness Rotator Cuff Tears

Most rotator cuff tears are said to start in the vulnerable zone in the anterior supraspinatus tendon close to the greater tuberosity of the humerus, while mid-substance tears that start more posteriorly are thought to be less frequent. However, recent work shows that most degenerate tears start close to the junction of the supraspinatus and infraspinatus tendons, about 15 mm posterior to the biceps tendon.[19] As tears enlarge, they extend proximally and/or in anterior or posterior directions and may eventually involve all the rotator cuff tendons and the biceps tendon.

Full-thickness rotator cuff tears extend all the way from the superficial or bursal surface of the tendon to the deep or articular surface, but not necessarily across the full width from front to back, whereas partial-thickness tears extend only part way between bursal and articular surfaces.

A defect that extends from the bursal surface to the joint surface of the tendon is the primary ultrasound sign of a full-thickness tear, and it should be present on both long-axis and short-axis scans of the tendon (Fig. 3.18). If an apparent defect is identified, the transducer should be angled to try to "fill in" the defect in case the appearance is due to anisotropy, and the defect should be shown on both longitudinal and transverse images. If the tear is very large and the tendon retracted under the acromion, no tendon is visible.

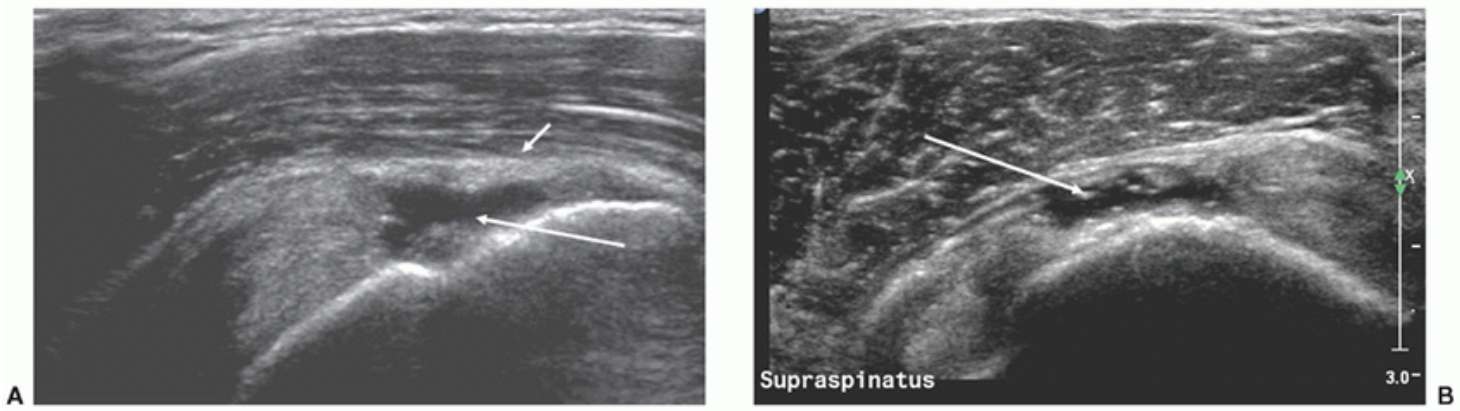

Figure 3.18. Long-axis (A) and short-axis (B) scans of small full-thickness supraspinatus tear. The defect is occupied by fluid (long arrows) and there is slight herniation of peribursal fat (short arrow in A) into the defect.

Tip:

Confirm a tear is present by showing a defect on both longaxis and short-axis images.

Fluid-filled defects are easy to identify because of the contrast differences between the fluid and the edges of the torn tendon, which may be slightly depressed. Tears are more difficult to identify if the fluid is echogenic or the defect occupied by synovium, debris, or by deltoid muscle (Fig. 3.19) that has herniated into the defect. Small tears can produce focal thinning or bursal surface depression indistinguishable from partial-thickness tears or severe tendinosis. Repeatedly pressing on the tendon with the transducer may move fluid or debris and make a small tear more obvious or distinguish a complete-thickness tear from a partial-thickness tear.

Tip:

Sonopalpation may make a tear more conspicuous or distinguish between full-thickness and partial-thickness tears.

Tear margins may be well defined or irregular. Delamination results in hypoechoic clefts that run transversely from the tear edge into the tendon. Rarely such a cleft communicates with a fluid-filled intramuscular cyst.

Tear extension >15 mm posterior to the anterior edge of supraspinatus tendon, which in practice is defined by the biceps tendon, indicates that the infraspinatus tendon is also torn. This measurement technique cannot be used if biceps is also torn, but the combination of biceps and supraspinatus tears usually indicates that the cuff tear is very large.

Tip:

Calculate supraspinatus tear width by measuring from the biceps tendon.

P. 33

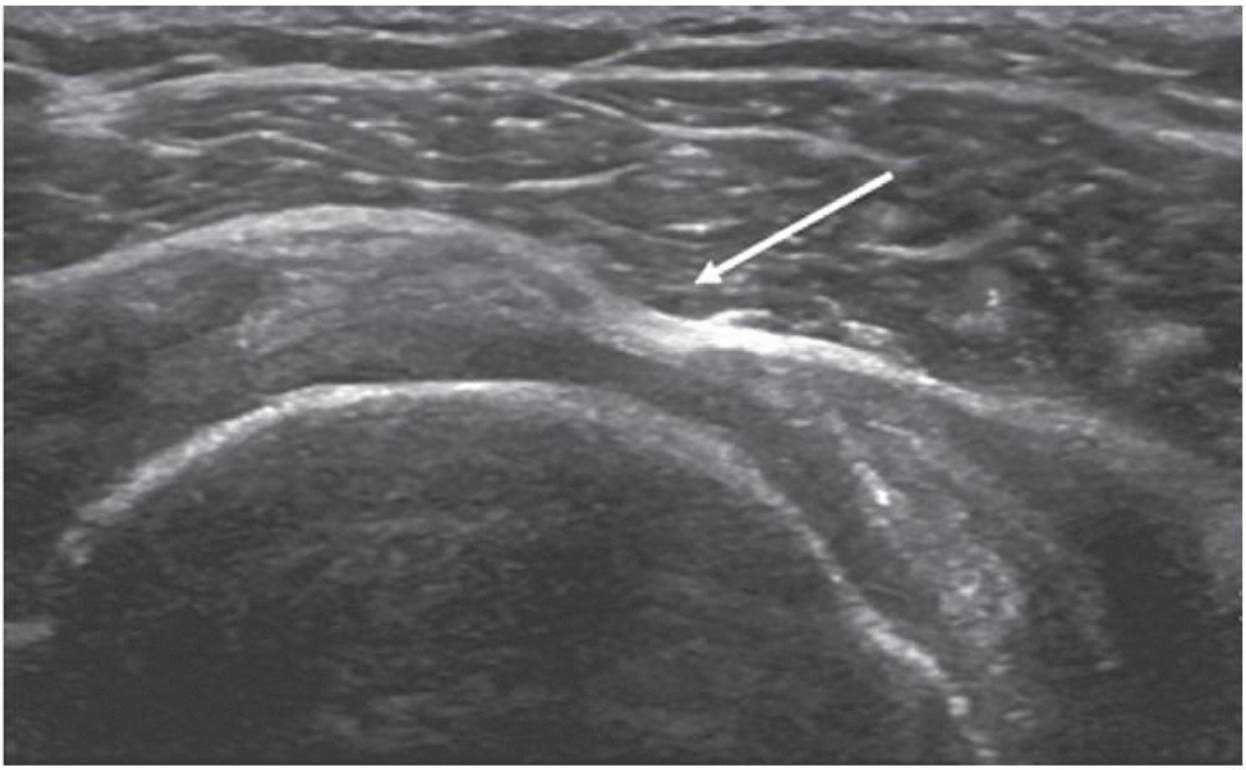

Figure 3.19. Short-axis scan of narrow full-thickness supraspinatus tear (arrow) with herniation of deltoid into defect.

Large tears result in tendon retraction under the acromion (Fig. 3.20), when the proximal edge of the tear cannot be seen. The deltoid muscle may herniate into the defect and be in direct contact with the humerus. It is important to recognise that there is a missing layer. Proximal migration of the humeral head to be in direct contact with the acromion (Fig. 3.21) occurs with very large chronic tears.

Full-thickness tears are associated with synovial inflammation[20] and abnormal signal is occasionally seen on Doppler ultrasound, but this is not a regular feature.

If a full-thickness tear is identified, the supraspinatus and infraspinatus muscles should be assessed for atrophy and fatty infiltration.

Secondary signs are highly suggestive of full-thickness tears but are not diagnostic. Depression or flattening of the bursal surface (Fig. 3.22) is a powerful indicator of pathology. It is nonspecific and occurs in both tears and tendinosis, although the deeper the depression, the more likely a full-thickness tear.

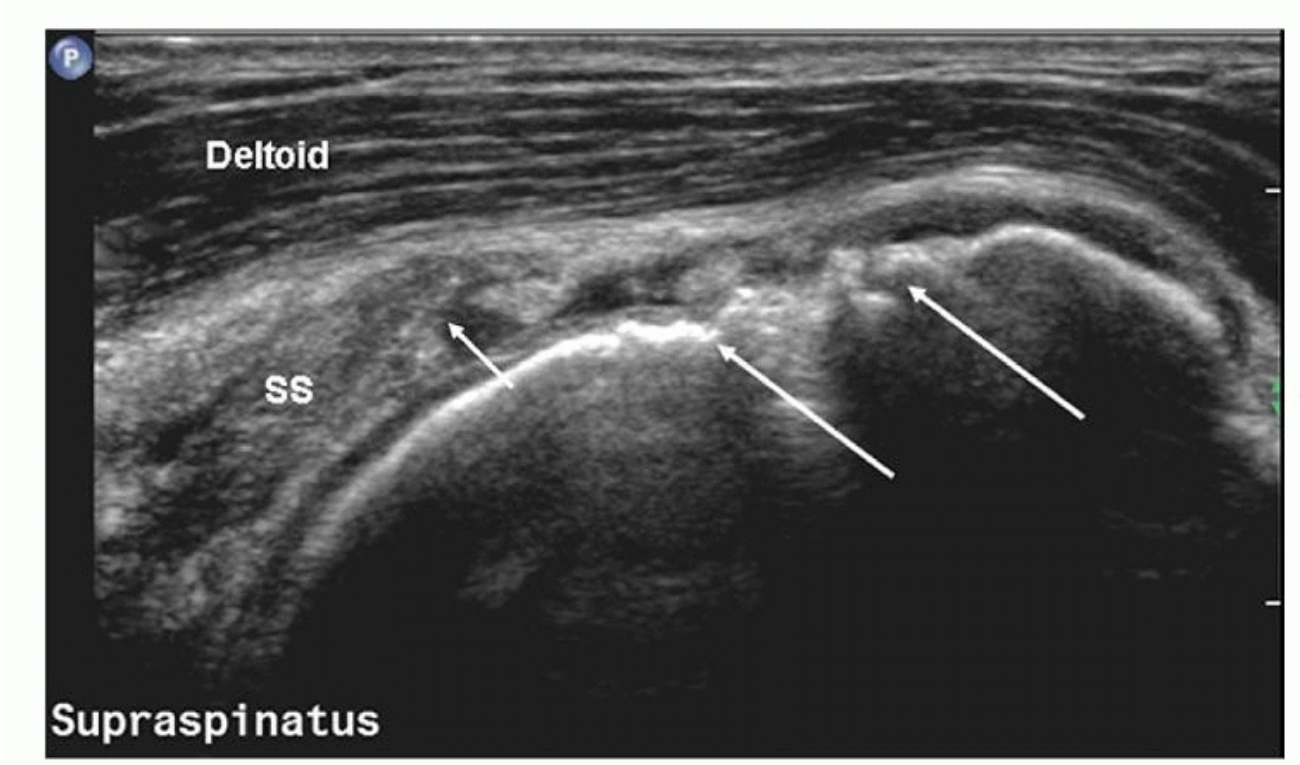

Figure 3.20. Long-axis scan of large full-thickness supraspinatus tear. The tendon is retracted (short arrow). Deltoid and fluid occupy the defect, and there is considerable hyperostosis on the humeral head (long arrow).

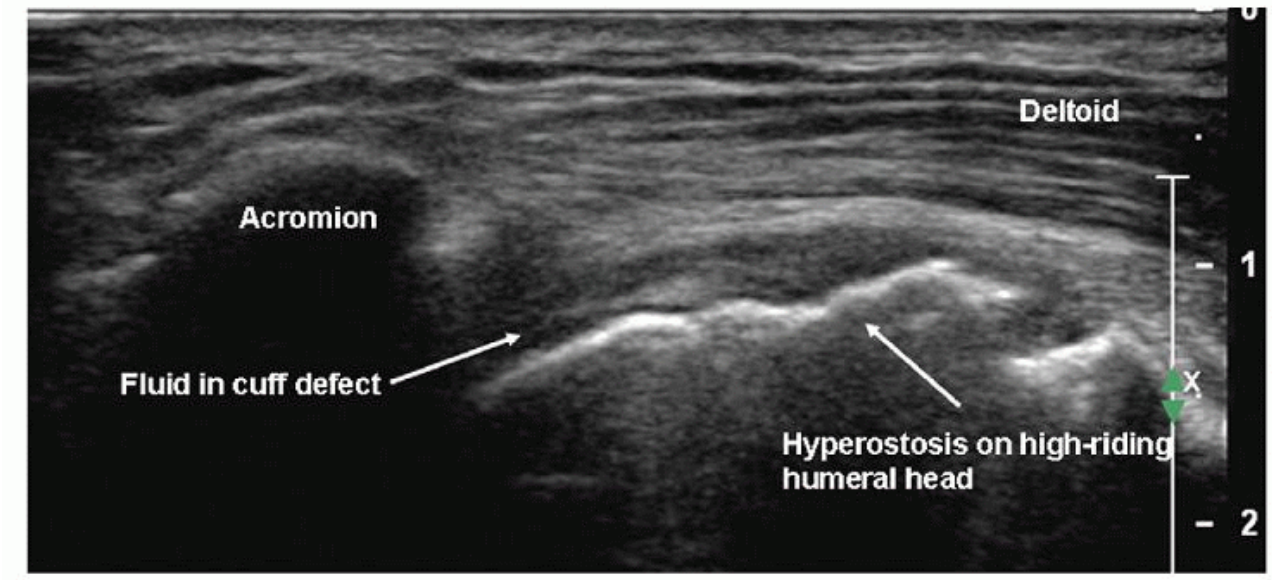

Figure 3.21. Massive rotator cuff tear. The cuff is retracted under the acromion, and the humeral head is high-riding.

Tip:

Bursal surface flattening or depression are sensitive indicators of cuff pathology, but are nonspecific.

The combination of glenohumeral joint fluid and hyperostosis at the greater tuberosity (Fig. 3.20) has a positive predictive value (PPV) and specificity of 100% for full-thickness tears. Fluid in the subdeltoid bursa and joint has a PPV of 95% and specificity of 99%. The bursa extends distal to the greater tuberosity (Fig. 3.23), and sometimes fluid is seen only in the distal segment. My experience is that fluid in the bursa and biceps tendon sheath also strongly suggests a tear, although a PPV of only 54% has been reported. Hyperostosis at the greater tuberosity or fluid in any one of the joint, bursa or biceps tendon sheath are less useful, having PPV value of 60% to 70%. A smooth tuberosity is likely to be associated with an intact tendon.[21,22,23,24]

The cartilage interface sign (Fig. 3.24) is an echogenic line at the surface of the hyaline cartilage on the humeral head deep to a cuff tear, and is due to reduced attenuation and altered acoustic interface. I do not find this a useful sign. The surface of the articular cartilage is often quite echogenic, especially with modern equipment, and

hyperechoity is subjective. In any case, the sign is frequently most conspicuous when there is an obvious tear and fluid is present.

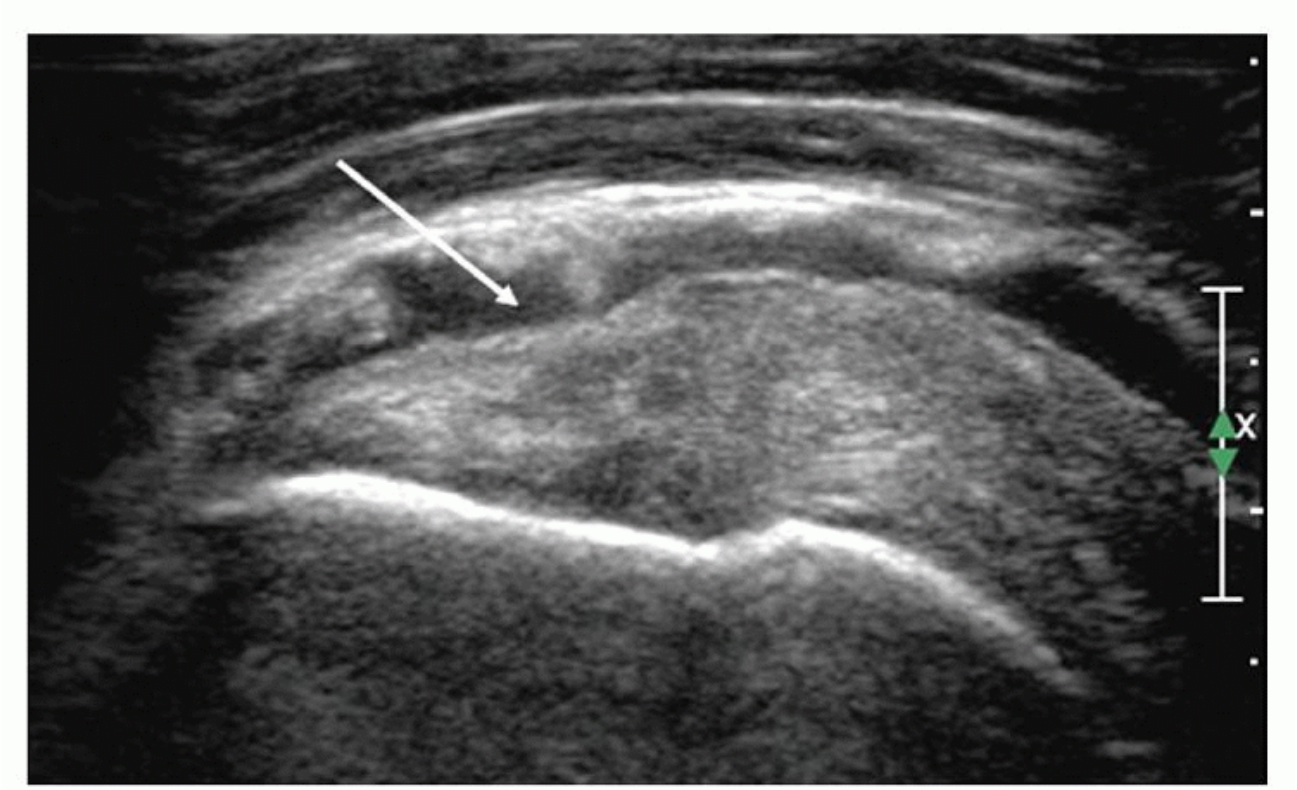

Figure 3.22. The effusion in the subdeltoid bursa shows that the bursal surface of supraspinatus is depressed (arrow).

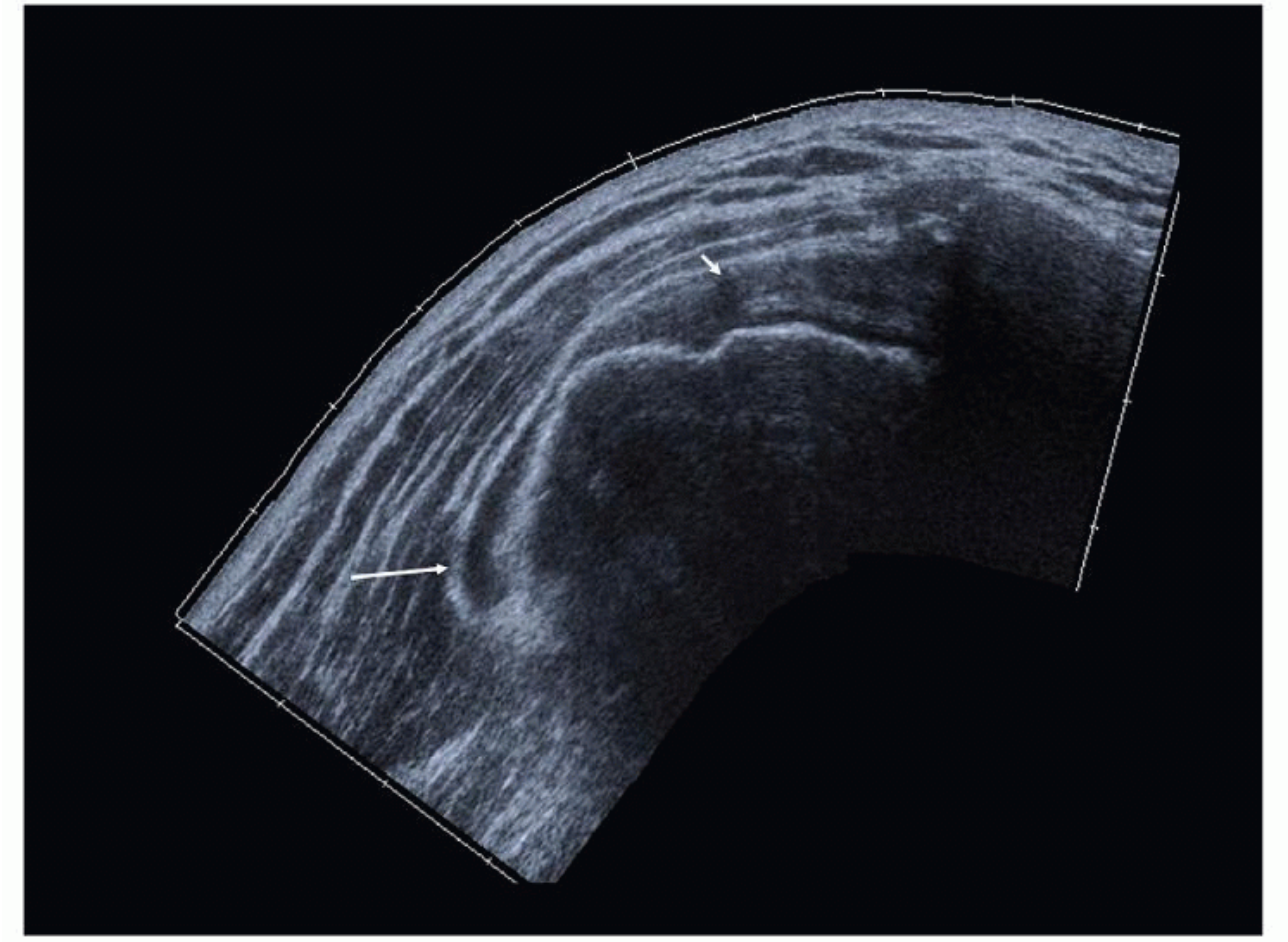

Figure 3.23. It is important to look quite far distally for bursal fluid. The fluid in this patient lies distal (long arrow) to the greater tuberosity of the humerus. There is no fluid overlying the rotator cuff (short arrow).

Tip:

These two combinations have high PPV for full-thickness rotator cuff tears:

- Hyperostosis at the greater tuberosity and fluid in the glenohumeral joint.
- 2. Fluid in the glenohumeral joint/biceps tendon sheath and subdeltoid bursa.

Partial-Thickness Rotator Cuff Tears

Partial-thickness tears extend part way between the bursal and the articular surfaces of the cuff and may be at the surface or intratendinous. Joint side tears are most common.[25]

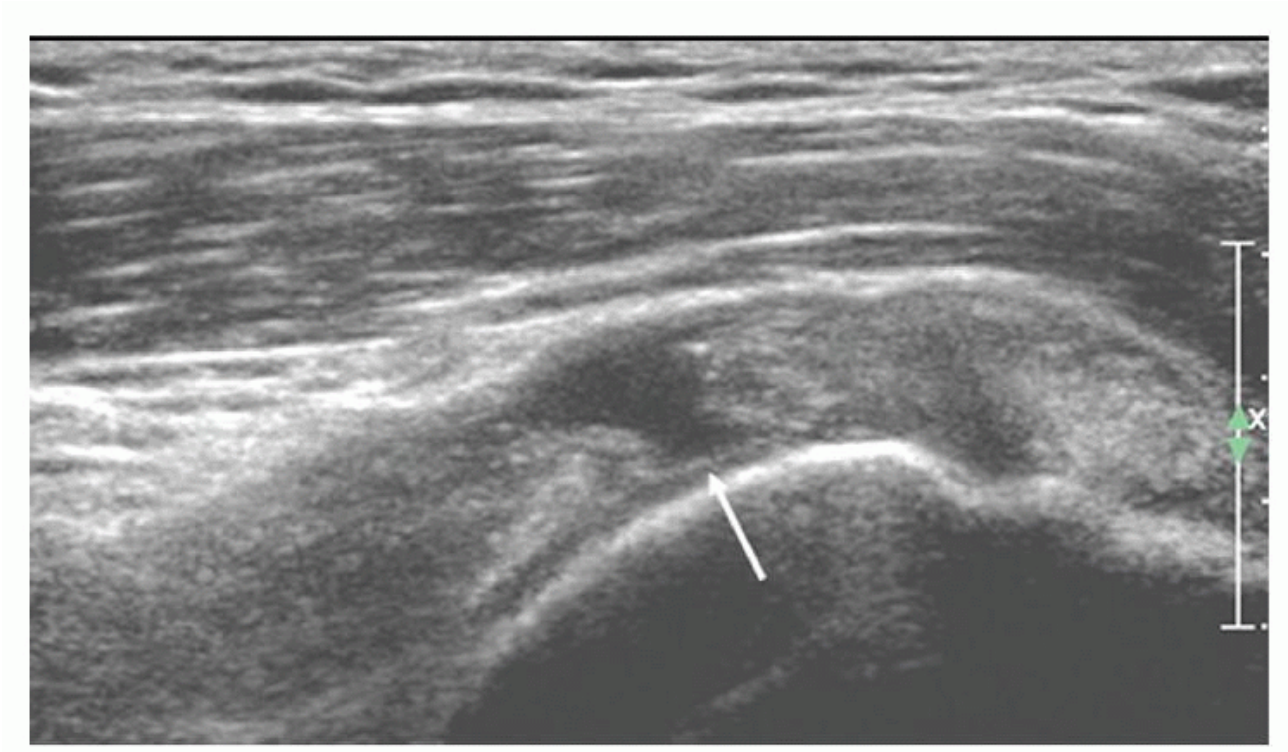

Figure 3.24. Articular cartilage (arrow) deep to a tear is brighter than adjacent cartilage.

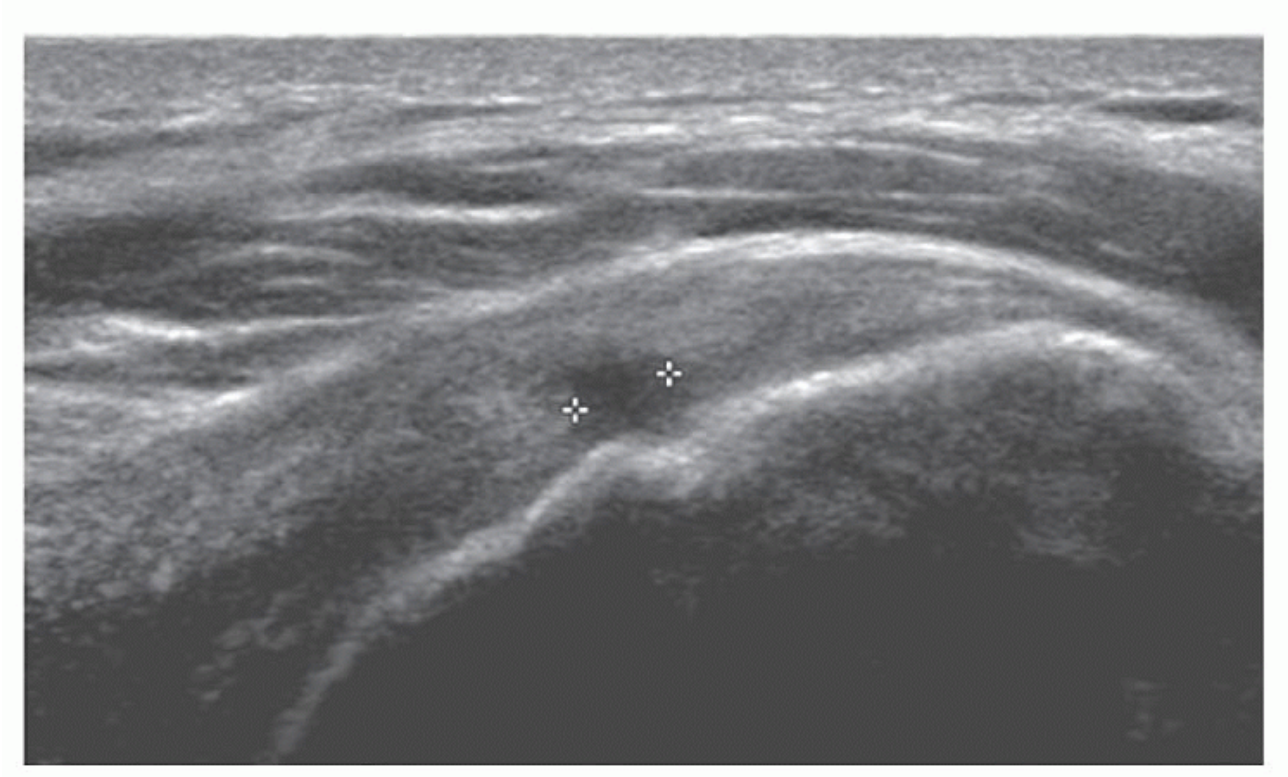

Figure 3.25. Joint side partial-substance tear between caliper marks.

Bursal-side tears cause defects or depressions (Fig. 3.22) in the bursal surface of the cuff, usually near the greater tuberosity. The bursa may dip into the defect and may be conspicuous because of intrabursal fluid or echogenic peribursal fat. Intrasubstance tears are hypoechoic. A longitudinal split in the tendon may be identified. Articular-side tears (Fig. 3.25) are easily identified if the defect is fluid-filled, but are frequently quite difficult to identify and may have a mixed hypoechoic and hyperechoic appearance.

Rim-rent tears (Fig. 3.26) are partialsubstance tears that are minimally retracted from the greater tuberosity and characteristically have a central echogenic “streak” surrounded by hypoechoic fluid.[26,27]

Rotator Cuff Tendinosis or Tendinopathy

Tendinopathy initially results in swelling and altered echogenicity. Swelling can be confirmed by comparing the affected segment with adjacent tendon or with the same position at the opposite shoulder. The difference in measurement is usually <2.5 mm. Thickness of >8 mm is also considered abnormal.[28]

Subsequently, the tendon may become thinned. Alterations in texture (Figs. 3.27 and 3.28) include reduced

P. 35

echogenicity, mixed hypoechoity and hyperechoity, and foci of microcalcifications (Fig. 3.29), although heterogeneity is often seen in older patients without clinical evidence of tendinosis. Thickening of the subdeltoid bursa and small amounts of fluid in the bursa may be present, and there may be subtle loss of definition between tendon and bursa.[24,28,29,30,31]

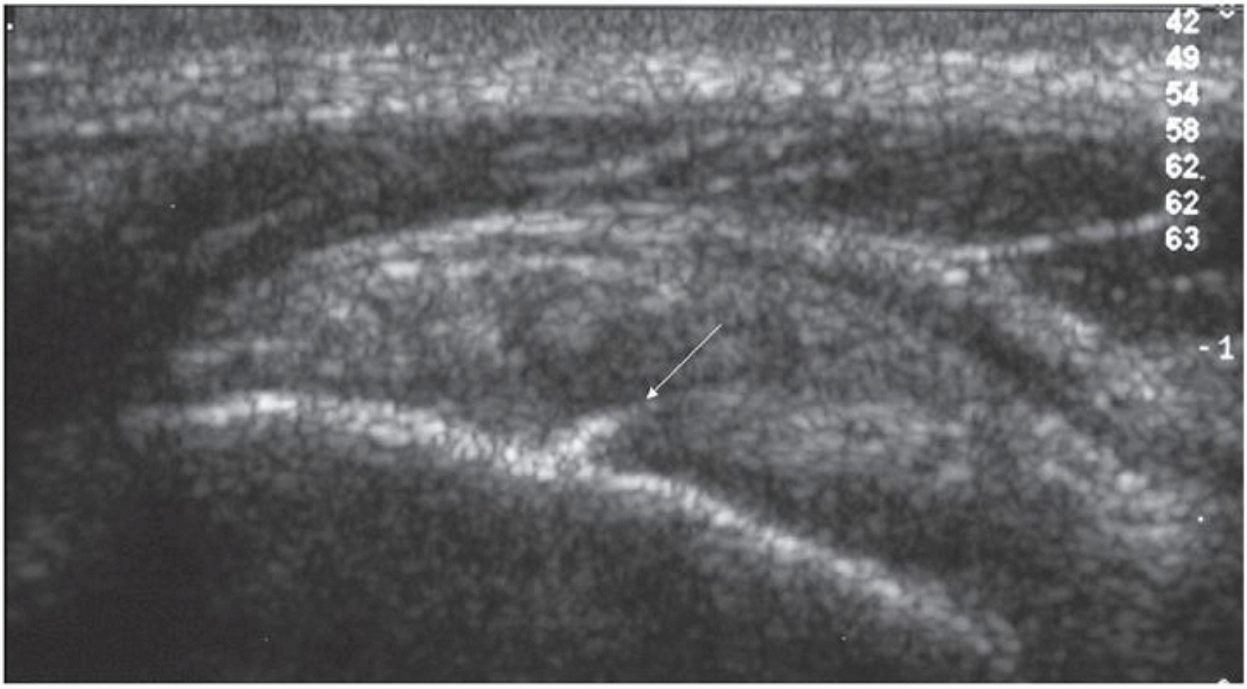

Figure 3.26. Echogenic streak (arrow) surrounded by hypoechoic fluid in supraspinatus adjacent to greater tuberosity typical of a “rim rent.”

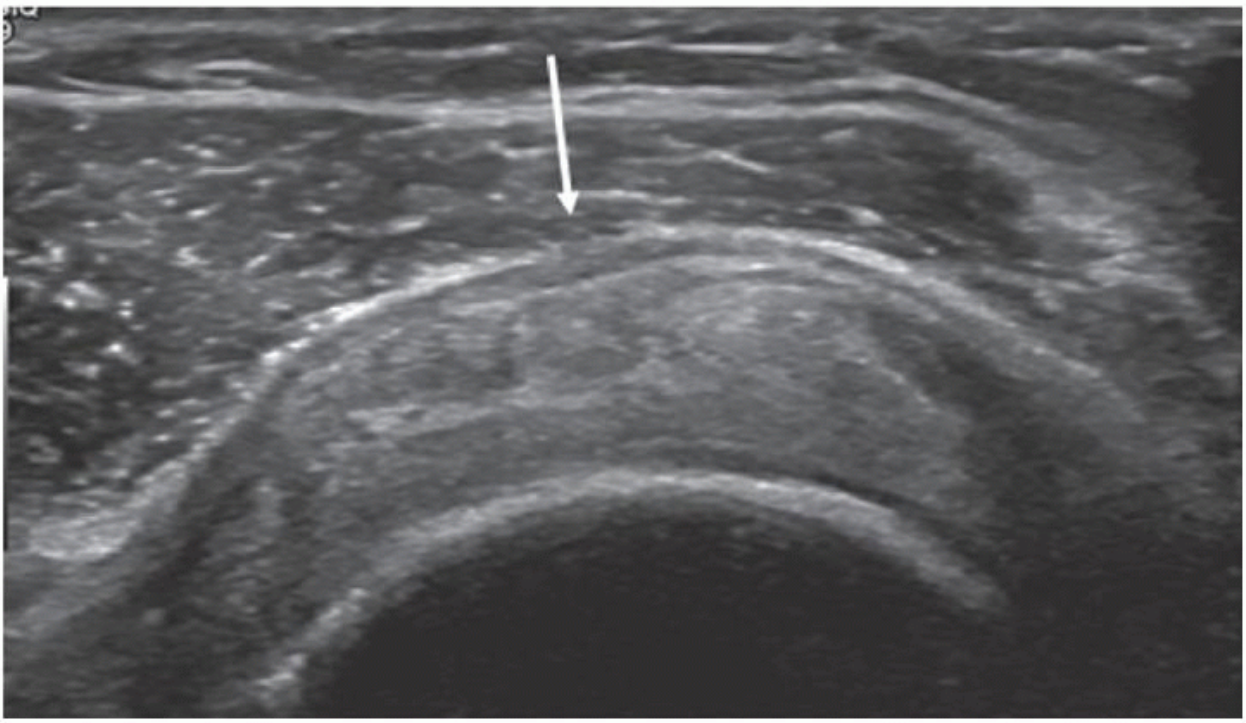

Figure 3.27. Supraspinatus tendinosis: the arrow points to bursal thickening, depression of the bursal surface of the tendon, and heterogeneous tendon texture.

Neer's theory postulates that increasingly severe grades of tendinosis develop into partial-thickness tears and then into full-thickness tears. Just as there are theoretical overlaps, there are overlaps between the ultrasound appearances of tendinosis and partial-thickness tears and between partial-thickness and full-thickness tears.

Accuracy of Ultrasound Detection of Rotator Cuff Tears

Ultrasound of the shoulder has been criticised as inaccurate and operator-dependent. Some initial reports recorded poor results. Subsequent studies have shown that there are no statistically significant differences between ultrasound and MRI in the detection of rotator cuff tears or the assessment of tear size compared with surgical results.[32],[33],[34] Performing MRI after normal ultrasound of the rotator cuff confers no benefit.[35]

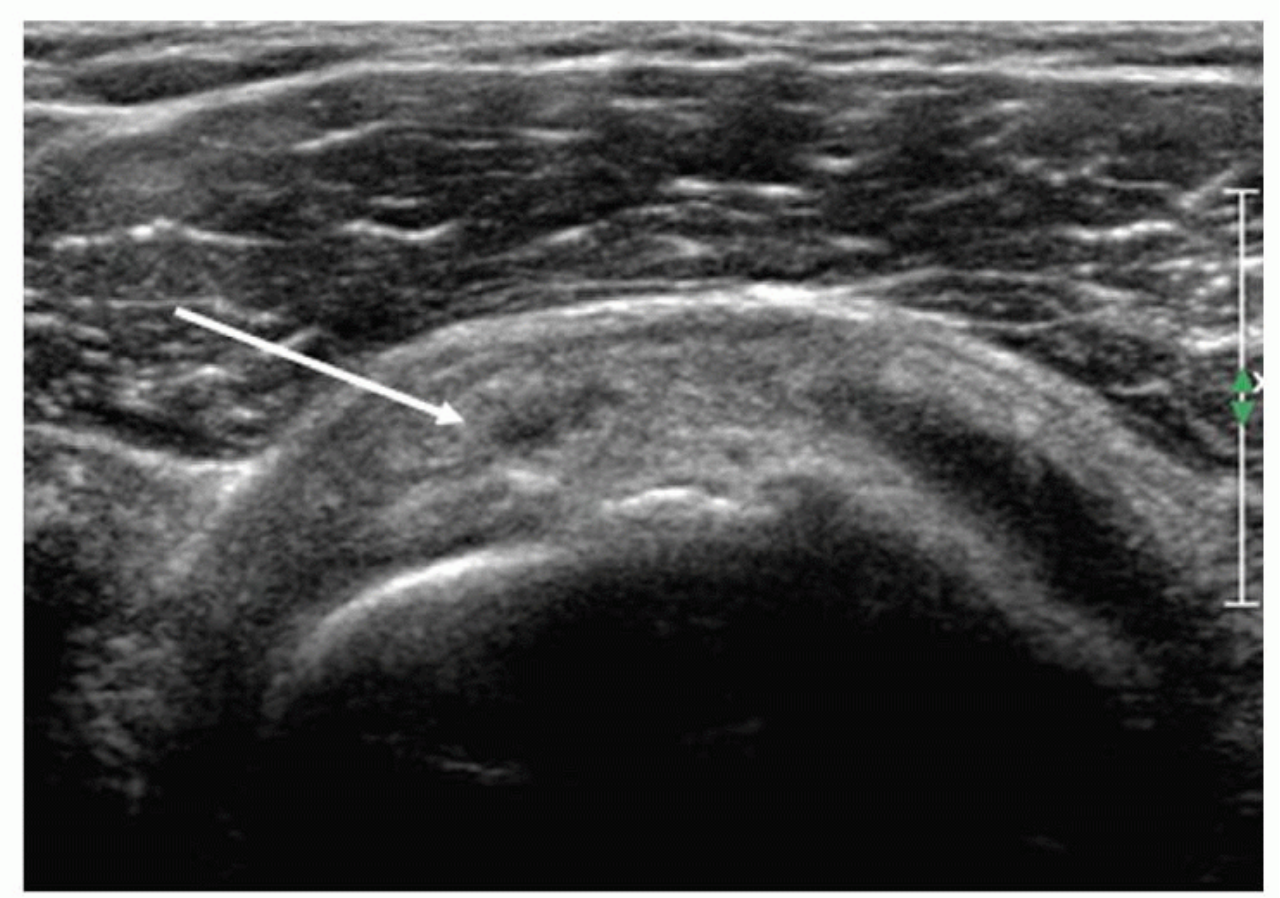

Figure 3.28. Supraspinatus tendinosis: the arrow points to an intrasubstance tear. The adjacent tendon is heterogeneous, and there is bursal surface flattening.

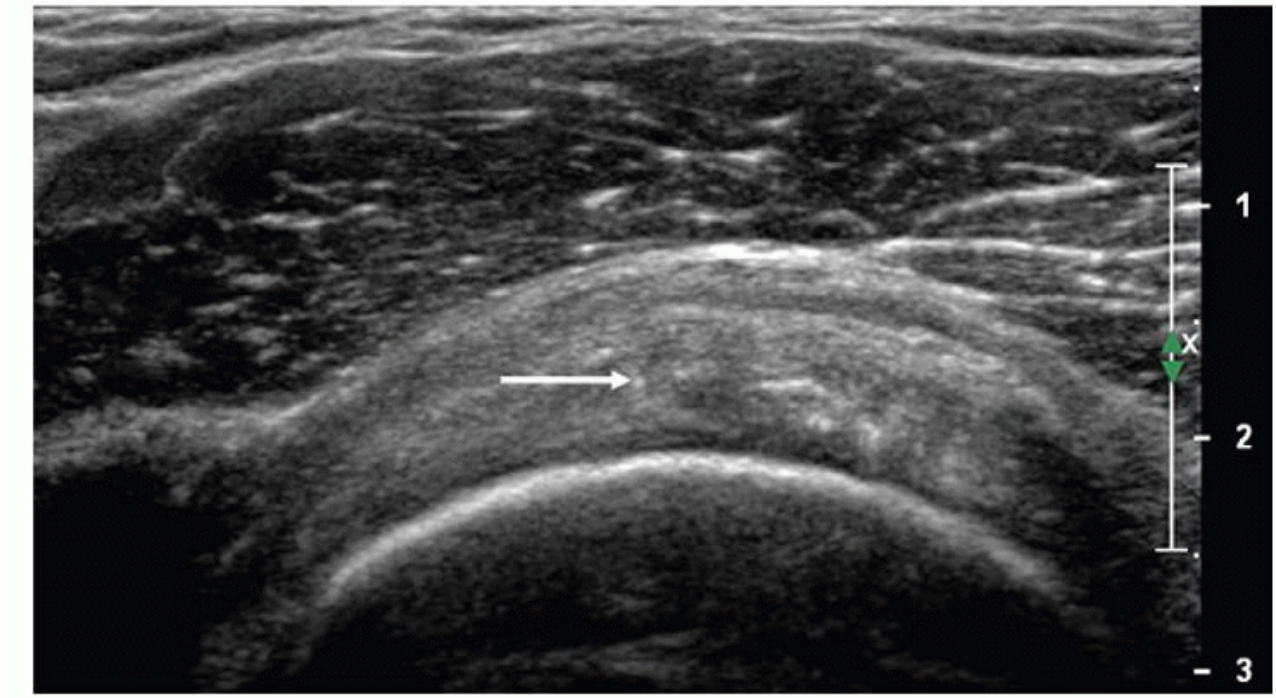

Figure 3.29. Short-axis scan of supraspinatus showing tendinosis. Microcalcification (arrow) and heterogeneous tendon texture are present.

A series of meta-analyses[1,18,36] has confirmed that ultrasound and MRI are equally accurate in the detection of rotator cuff tears, although results for both modalities are poorer for partial-thickness tears than full-thickness tears, and MR arthrography is a more accurate technique by a very small margin (Table 3.1).

Ultrasound errors include simple misses, usually of very small (<5 mm) tears, miscategorisation between fullthickness and partial-thickness tears or between partialthickness tears and tendinosis, and when patients are too big (heavily muscled or obese) or have such a restricted range of movement that parts of the rotator cuff are inaccessible.[37]

TABLE 3.1. Accuracy of Imaging in Rotator Cuff Tears

	Sensitivity (%)	*Specificity (%)*
FULL-THICKNESS TEARS		
MRA	95.4	98.9
US	92.3	94.4
MRI	92.1	92.9
PARTIAL-THICKNESS TEARS		
MRA	85.9	96.0
US	66.7	93.5
MRI	63.6	91.7

MRA, magnetic resonance arthrogram; US, ultrasound; MRI, magnetic resonance imaging.

(Adapted with permission from de Jesus JO, Parker L, Frangos AJ, et al. Accuracy of MRI, MR arthrography, and ultrasound in the diagnosis of rotator cuff tears: a meta-analysis. *AJR Am J Roentgenol.* 2009;192(6):1701—1707; Published with permission from Beggs I. Shoulder ultrasound. *Semin Ultrasound CT MR.* 2011;32(2):101-113.)

P. 36

There is no doubt that partial-thickness tears are more difficult to diagnose than full-thickness tears.[38] Large bursal-side partial-thickness tears may be indistinguishable from full-thickness tears. When faced with this dilemma, I report frankly that I cannot make the distinction, and the surgeon will usually operate. In some cases, the difficulty is in distinguishing between tendinosis and partial tears, but as the management of both conditions is initially conservative, this is not usually of major practical significance. Subacromial decompression is performed if conservative treatment of impingement fails and debridement of partial tears can be performed at that time.[25,37]

Discrepant results have been found for tear measurement. Teefey et al.[32] found that ultrasound correctly assesses length in 73% and width in 86% of full-thickness tears compared with surgical measurements. Discrepancies are three times as likely to overestimate as underestimate tear length while over- and underestimates are equally likely when measuring width.[32] Curved measurements are more accurate than straight line measurements.[39] Tissue harmonic imaging improves image quality and may also help.[40]

The miscalculation of tear length is partly, not wholly, attributable to non-visualisation due to retraction under the acromion, as similarly poor results occur with MRI. Discrepancies may be due to the position of the shoulder when the tear is measured. Ferri et

al.[41] found no differences between ultrasound and surgical measurements in full internal rotation ("hand-behind-the-back position") but lesser degrees of internal rotation ("hand-in-backpocket position") underestimated tear length.

Tip:

Measure rotator cuff tear size with the patient in the "handbehind-the-back" position.

The criticism that shoulder ultrasound is operatordependent usually comes from surgeons, as if their own work is not operator-dependent. Standard clinical tests for rotator cuff pathology have sensitivities of 23% to 76% and specificities of 47% to 88% and are subject to considerable inter-observer variability, and it would be strange to think that there are not also variations in surgical results.[5,17,42]

In experienced hands, ultrasound has high (>90%) inter-observer agreement. Most significant discrepancies concern the distinction between full-thickness and large partial-thickness tears or whether a supraspinatus tear extends into the infraspinatus.[43,44,45] Interobserver agreement improves with experience.[45] The learning curve is usually considered to be quite lengthy. However, Rutten et al.[46] showed excellent agreement between an experienced musculoskeletal sonologist and an experienced abdominal sonologist with no prior musculoskeletal experience.

Several surgeons have reported their experience of performing ultrasound with little or no training, although in many cases they interpreted the ultrasound only after examining the patient and previous imaging studies. Moosmayer,[47] a surgeon, reported excellent results unbiased by any clinical information, but had already performed several hundred shoulder ultrasound examinations by the start of his study.[48] Hedtmann and Fett[48] also reported excellent results after extensive training. Good results have prompted some surgeons to perform their own ultrasound examinations as part of a "one-stop shop" shoulder clinic.[3,34]

Asymptomatic Rotator Cuff Tears

The reported prevalence of asymptomatic rotator cuff tears over the age of 50 ranges from 6% to 40%, and increases with age to 51% at 80 years or older. Although patients are pain-free, objective testing shows reduced shoulder strength, especially when the tear is large.[49,50,51,52,53] About half of the patients become symptomatic within 3 years. About one-third show tear progression, and most of these become symptomatic.[54] Symptomatic rotator cuff tears are associated with rotator cuff tears on the opposite side. These may or may not be asymptomatic; 56% of patient had a tear in the opposite asymptomatic shoulder in one series.[55]

It follows that many patients who present with an injury and are found to have a rotator cuff tear may have a long-standing, previously unrecognised tear, and immediate tendon repair may be inappropriate. A massive tear, paucity of fluid, hypertrophied biceps tendon, high-riding humeral head, and muscle atrophy and fatty infiltration are all features of chronic tears.[56,57]

Tip:

A massive tear, no fluid, thick biceps, high humerus, and fatty muscle indicate long-standing tear.

Muscle Atrophy and Fatty Infiltration

Atrophy and fatty infiltration of the rotator cuff muscles are frequent consequences of rotator cuff tears and may affect the functional outcome of tendon repair, and hence the decision to operate or the type of surgery performed. Fatty atrophy is not an inevitable consequence of a rotator cuff tear, but the larger the tear the greater is the degree of fatty infiltration likely to be.[58]

Infraspinatus atrophy is commonly seen when the supraspinatus tendon is torn and infraspinatus appears intact. This apparent paradox may be explained by the finding that the infraspinatus footprint is much larger and extends more anteriorly than previously thought. A tear that apparently involves only supraspinatus may therefore also involve infraspinatus.[5]

The "tangent sign" assesses supraspinatus atrophy on sagittal oblique computed tomography (CT) and MRI

images of the supraspinatus fossa by drawing a line across the superior margins of the coracoid process and the spine of the scapula. A similar tangent line assessment can be performed on sagittal oblique ultrasound scans. Supraspinatus is considered to be atrophic if it does not reach the tangent line (Fig. 3.30). This finding correlates with objective measurements of muscle strength and the occupancy ratio measure of atrophy.[59,60] The occupancy ratio is calculated on sagittal oblique images at the level of the suprascapular notch by drawing separate ellipses around the margins of the muscle and the fossa. Supraspinatus is considered normal if it occupies 0.6 to 1.0 of the fossa, moderately atrophied if 0.4 to 0.6, and severely atrophied if <0.4.[61,62]

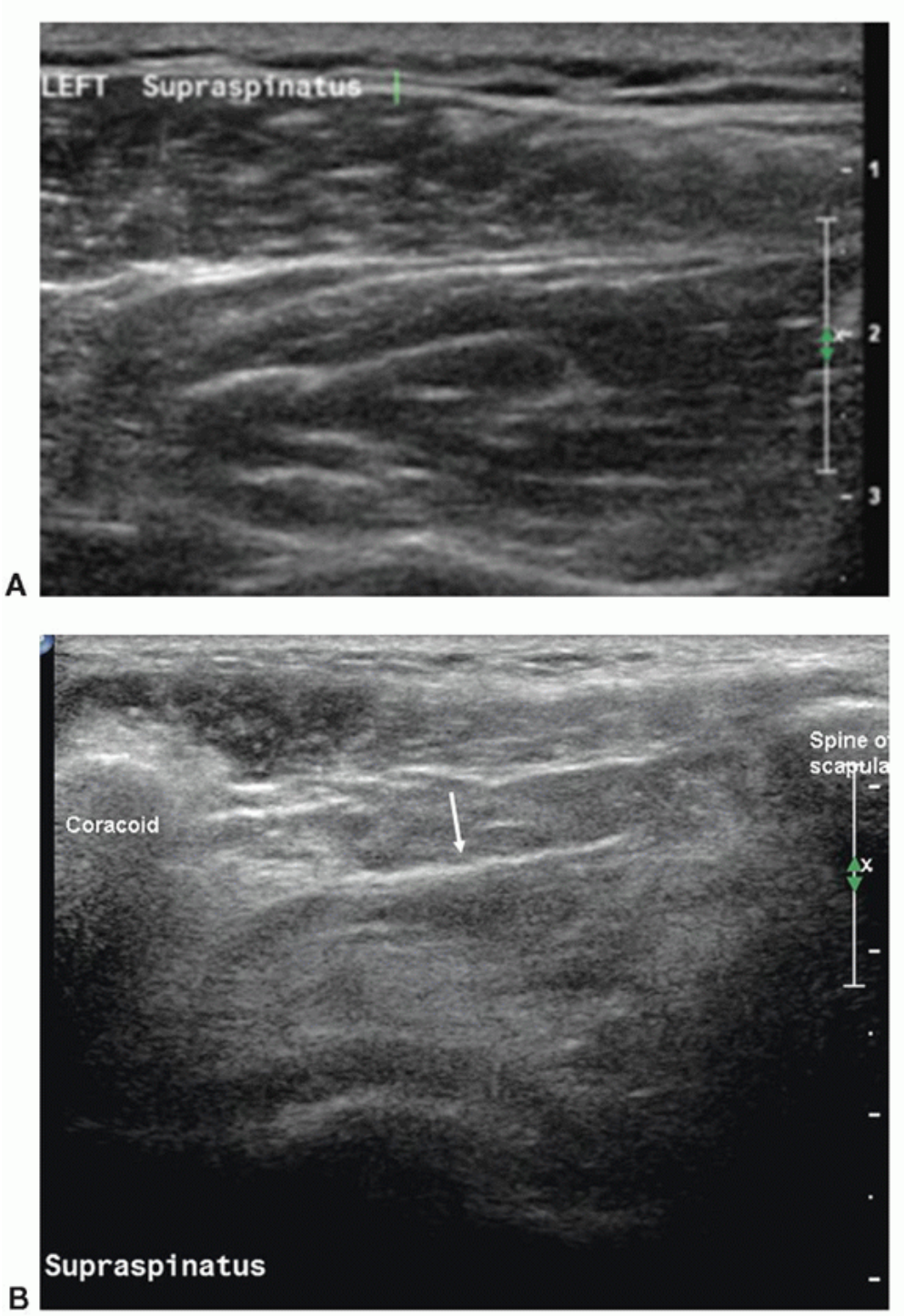

Figure 3.30. A: Sagittal scan of supraspinatus fossa showing normal architecture and bulk of supraspinatus muscle. B: Sagittal scan of supraspinatus fossa showing atrophy and fatty infiltration of supraspinatus muscle. The superficial surface of supraspinatus normally reaches a line between the coracoid process and the spine of the scapula. In this case the superficial margin of the muscle (arrow) lies deep to the line, indicating that the muscle is atrophic. The muscle is diffusely echogenic and has lost its internal architecture in keeping with fatty infiltration.

CT and MRI grading systems show that muscles that contain no fat or streaks of fat have good functional outcomes after rotator cuff repair, while muscles that contain more fat (Grade 2, “fat less than muscle” or greater) have poor outcomes.[61,63,64,65,66,67] Scattered deposits of fat result in increased echogenicity of the muscle and loss of definition of its contour, pennate pattern, and central tendon (Fig. 3.30). Increased echogenicity is easily recognised by comparing supraspinatus or infraspinatus with the overlying deltoid or trapezius muscles (Fig. 3.31), which also helps to distinguish between normal age-related atrophy and atrophy from a rotator cuff tear. The ultrasound grading of fatty infiltration is subjective, but a muscle that is clearly

more echogenic than the overlying deltoid has a substantial degree of fatty infiltration, equivalent to at least Grade 2 on MRI or CT. Assessment of infraspinatus is easier than supraspinatus and can be aided by extended-field-of-view imaging.[62,68,69]

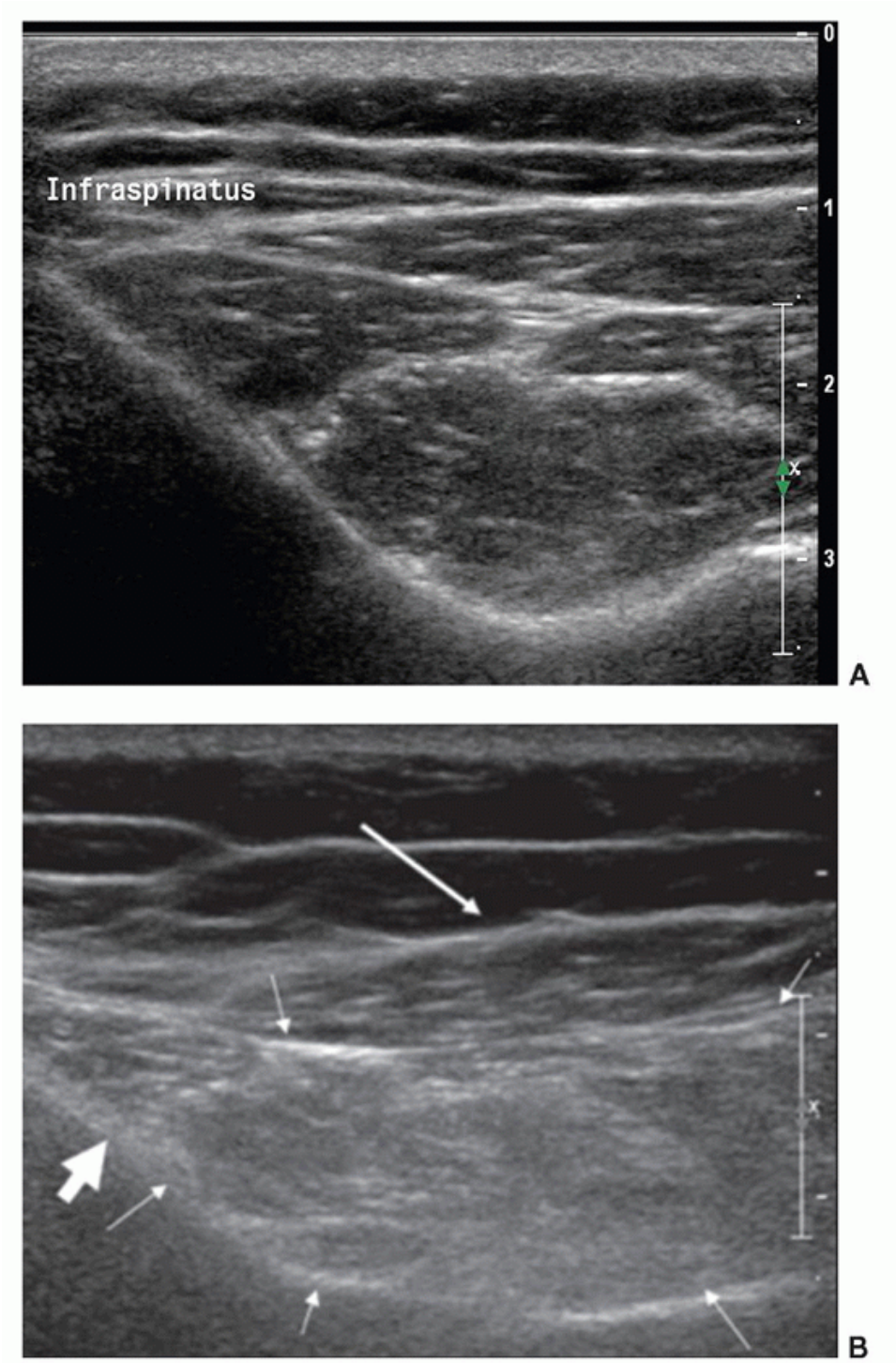

Figure 3.31. Sagittal scans of infraspinatus muscle (short arrows in B). The scapula (broad arrow in B) is deep and trapezius (long arrow) is superficial. A: Normal infraspinatus muscle that is isoechoic to trapezius and has well-defined internal architecture. B: Fatty atrophy. The muscle is diffusely more echogenic than trapezius, is reduced in size, and has lost its internal architecture.

Tip:

Fatty infiltration is easily identified by comparing the echogenicity of infraspinatus and the overlying deltoid or trapezius muscles.

Impingement

Most cases of rotator cuff impingement are anterosuperior and involve the supraspinatus tendon and the coracoacromial arch. Extrinsic etiological factors include the morphology of the arch, repetitive and tensile overload, and biomechanical factors, while intrinsic factors include tendon vascularity. It is now accepted that changes at the coracoacromial arch are also consequences of impingement.[6,70]

Neer described three progressive stages of tendon abnormality as a result of impingement. Stage I, characterised by subacromial bursitis and minor or no tendon changes, is reversible. Stage II additionally shows evidence of irreversible tendinosis and may require decompression of the coracoacromial arch to halt progression and relieve symptoms. Stage III damage includes partial-thickness and full-thickness tears and may need decompression and tendon repair.[13]

Clinical features of impingement include pain, particularly on overhead movement, stretching, or internal rotation, painful arc, pain that disturbs sleep and localised tenderness over the greater tuberosity. Radiographs may show hyperostosis at the greater tuberosity and spurs on the acromion.

Clinical tests of impingement are widely used but are, at least in some cases, of doubtful validity.[16]

A widely used clinical test is to inject local anesthetic into the subacromial bursa to try to abolish pain and a painful arc. Long-acting steroids may be added for therapeutic purposes. Blind injections into the bursa may be accurate in experienced hands,[71] but most studies show that "blind" injections frequently miss the bursa and may result in a false negative "impingement test."[72,73,74,75,76]

Ultrasound-guided bursal injections (Fig 3.23) are widely used for both diagnostic and therapeutic purposes. In addition to the evidence that ultrasound-guidance ensures accurate needle placement, it seems intuitively reasonable to assume that intrabursal injections will improve therapeutic response and there is evidence to support this.[77] However, a double blind study failed to show any benefit for ultrasound-guided bursal injections over blind gluteal injections of steroid.[78]

Ultrasound evidence of impingement includes bursal thickening and rotator cuff damage (Fig. 3.27). Dynamic scanning is performed during active or passive abduction. Passive abduction is easily achieved if the examiner grasps the patient's flexed elbow and abducts the arm. Alternatively, the patient is asked to abduct the arm. Abduction in internal rotation and 60° forward flexion may help. The transducer is placed on the edge of the acromion and CAL, parallel to the long axis of supraspinatus. Ultrasound shows pooling of bursal fluid or buckling of the bursa or bursal surface of the cuff against the acromion or CAL (Fig. 3.32). In more severe cases, the greater tuberosity of the humerus may block against the acromion. However, these findings have not been objectively verified, and pooling of bursal fluid or buckling of the bursa may be seen in asymptomatic patients.[28,29,30,79]

My own preference in assessing impingement is to perform ultrasound-guided bursal injections. I use a combination of 1mL of 1% lidocaine and 5mL of 0.5% bupivacaine, which are short-acting and long-acting local anesthetics, respectively and monitor response by asking the patient to subsequently complete a VAS (visual analogue pain score) at hourly intervals, although in most patients a positive response (or its absence) is obvious almost immediately. I also inject 40 mg of methylprednisolone, a long-acting steroid, for possible longer-term benefit. I prefer methylprednisolone because of its reduced risk of skin depigmentation but others prefer triamcinolone because of its reduced risk of causing synovitis.

I perform the injection with the patient supine to avoid a vasovagal reaction. The patient's hand is usually in a neutral position by the patient's side but sometimes a degree of internal or external rotation is needed to visualise the bursa optimally. I scan along the long-axis of supraspinatus to identify the bursa and mark the skin so that the needle will run (from inferolateral to superomedial) as close to parallel to the transducer as possible. After cleaning the skin and injecting subcutaneous local anaesthetic I insert a green needle attached to a 5mL syringe loaded with local anaesthetic. The bevel of the needle should point down. The needle is then inserted into the bursa and a small test dose of local anaesthetic is injected. If the needle is in the bursa, the sensation when injecting is like a "knife through

butter" and there is very little to see as the injected fluid runs away from the needle tip into the bursa. Pooling of fluid around the needle tip indicates that the needle is outside the bursa and the needle should be repositioned. Occasionally intrabursal adhesions are present and the bursa has to be 'forced' to distend by pushing harder on the syringe but care must be taken to ensure that the injection is truly intra-bursal. After distending the bursa with local anaesthetic, the steroid is injected. I tell patients that they might experience 2 to 3 days of modest discomfort after the injection but warn them that severe pain due to a steroid 'flare' is a possibility. I ask them to avoid strenuous activities and to refrain from physiotherapy for 2 to 3 weeks after the injection. My experience is that about 60% of patients still benefit 6 months after injection.

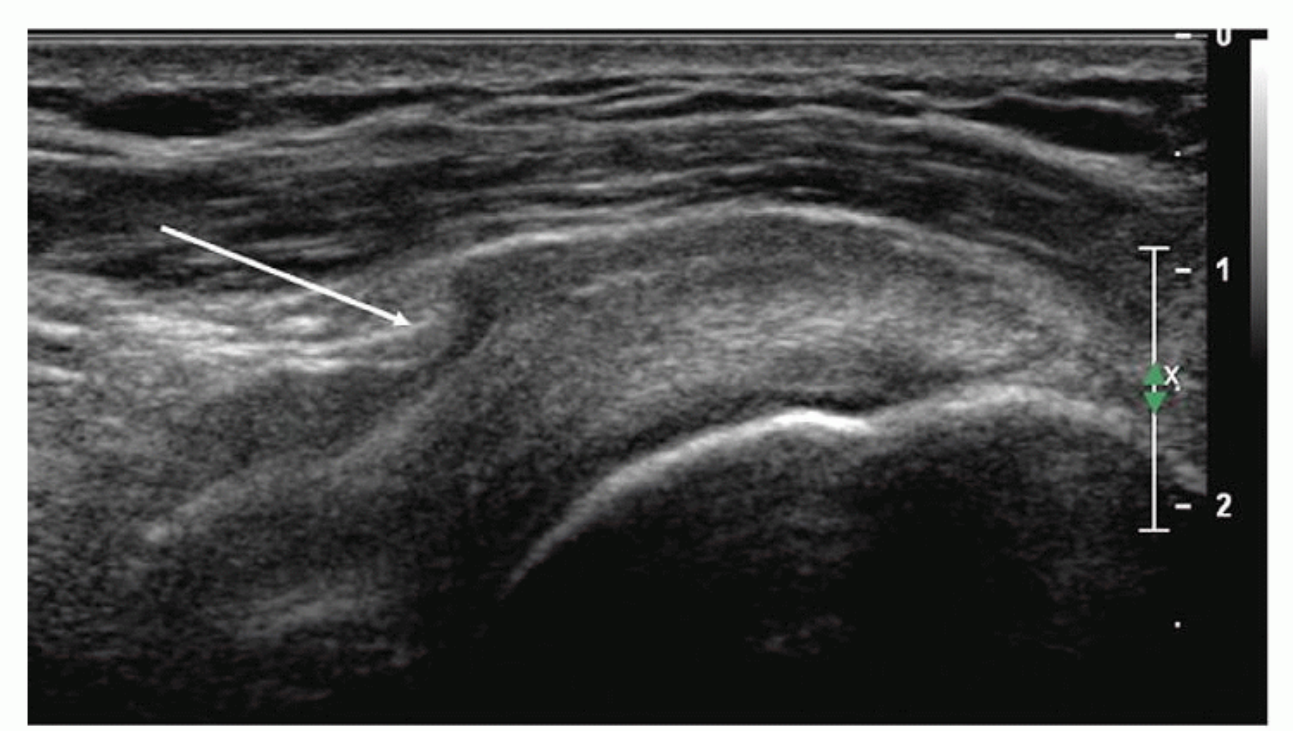

Figure 3.32. Rotator cuff impingement: the bursa is thickened and the CAL (arrow) protrudes into the bursa.

Frozen Shoulder

Frozen shoulder or adhesive capsulitis results in stiffness, globally restricted range of active and passive movement, and severe pain that disturbs sleep. Patients are middleaged, often diabetic. The cause of frozen shoulder is unknown. Arthroscopy shows fibrous soft tissue thickening in the rotator interval, particularly around the CHL.[80,81] Inflammation is not a feature of established disease, but synovial inflammation may be present initially.[82] Frozen shoulder is usually a clinical diagnosis that does not require imaging.

Ultrasound shows increased soft tissue density in the rotator interval, thickening of the CHL, and vascularity in the rotator interval on Doppler imaging. Restricted abduction is seen during dynamic examination, but this is obvious clinically. Magnetic resonance arthrography shows changes in the rotator interval including thickening of the capsule, synovium, and CHL.[83,84,85]

Frozen shoulder is a self-limiting condition that has a protracted course and may last several years. Complete functional recovery may never be achieved. Image-guided intra-articular steroid injections may help, although severe or recalcitrant cases may require operative intervention.[81,86] I use fluoroscopy to perform image-guided injections for frozen shoulder but ultrasound - guidance can be employed. An identical ultrasound technique can be used to inject contrast for MR arthrography or to aspirate the joint for organisms or crystals. The patient either sits on the examination couch or lies semiprone, facing away from the operator, with the hand on the opposite shoulder. The infraspinatus muscle/tendon and underlying posterior gleno-humeral joint line are identified by placing the transducer obliquely on the posterior shoulder with the outer end of the transducer rotated superiorly and the skin is marked for either an inferomedial to superolateral needle trajectory or the reverse trajectory. After skin preparation, including infiltration with local anaesthetic, a 22G spinal needle is advanced under ultrasound guidance towards the posterior glenohumeral joint line and the posterior aspect of the humeral head. When it touches bone a small test injection of anaesthetic is made to show if the needle is in joint or has to be repositioned. If the needle is intra-articular, I then inject 40 mg of triamcinolone, 5mL of 0.5% bupivacaine and 15 mL of air or normal saline to distend the joint. The purpose of the injection is to alleviate pain and to restore the range of joint movement and all of my patients receive physiotherapy within a few days of the injection, although the evidence for the efficacy of post-injection physiotherapy is mixed. Audit shows that 70 to 80% of patients benefit from the procedure. As with all intra-articular steroid injections, I warn patients to expect mild discomfort or pain and the possibility of severe pain due to a “steroid flare” in the next 2 to 3 days.

CALCIFICATION

Deposits of calcium hydroxyapatite in the rotator cuff include foci of microcalcification that are radiographically occult, and larger “hard” or “soft” deposits that are visible on radiographs. Supraspinatus is the most frequent site, but any of the tendons may be involved. The cause remains unknown although hypoxia and metaplasia have been suggested. Large foci of calcification are initially hard and often clinically occult, although chronic pain may subsequently develop. After a latent period, which is often prolonged, an inflammatory resorptive phase follows and the calcium softens or fragments. This phrase often causes severe pain and lasts for several weeks. As the overlying skin may be hot and erythematous and inflammatory markers are elevated, patients are often thought to have septic arthritis and are referred for urgent ultrasound and aspiration. Rupture of calcium into the subdeltoid bursa may result in bursitis and exacerbation of pain or more frequently relieve pain, presumably by reducing the pressure and inflammation in the tendon. Rarely, calcium may extend into the humerus or rupture between the tendon and the bursa.[87]

Microcalcification produces small echogenic foci (Fig. 3.29) in the rotator cuff that are usually seen in the context of tendinosis. Acoustic shadows are infrequent. Distinguishing microcalcification in the tendon from hyperostosis on the cortex may be impossible if the echogenic focus is adjacent to the bone.

Most large calcifications are hard and have a densely echogenic convex superficial surface (Fig. 3.33). Multiple foci may be present. Distal acoustic shadowing is typical unless the calcification is too close to the humerus for shadowing to be seen. Rotator cuff tears and abnormal signal on Doppler ultrasound are rare. Deposits occasionally elevate the bursal surface of the tendon, causing pain on abduction when the bursa impinges on the acromion.

Soft calcification is often exquisitely painful and tender. Even gentle transducer pressure may be very uncomfortable. Soft calcification (Fig. 3.34) is less echogenic

P. 40

than hard calcification and may be difficult to see if it is almost isoechoic with the tendon. Acoustic shadowing is uncommon. Hyperaemia (Fig. 3.35) in and around the calcification on Doppler ultrasound is associated with pain and a good response to needling. If the patient can tolerate it, increased transducer pressure may show fluid movement within the calcium deposit. Rupture into the subdeltoid bursa leaves echogenic streaks of calcium in the tendon and fluid and increased echogenicity in the bursa.

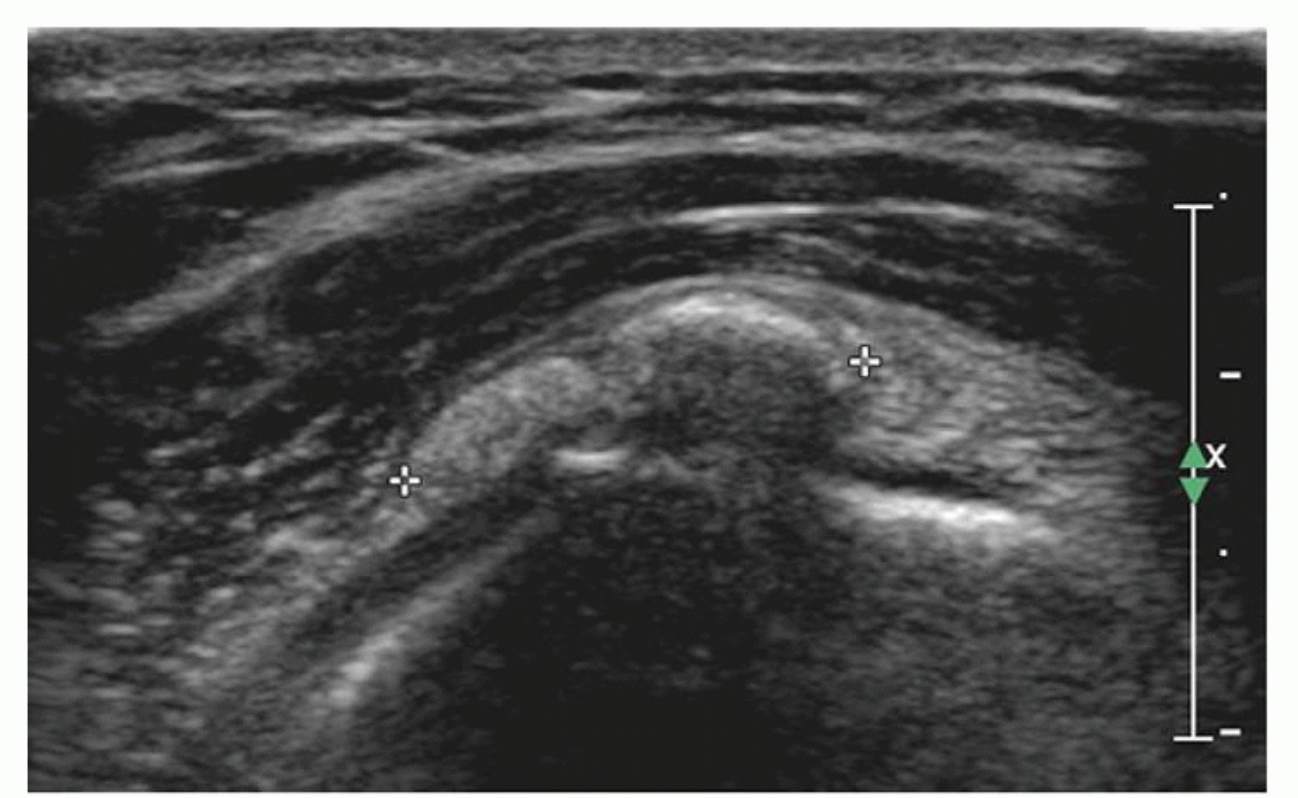

Figure 3.33. Large dense focus of “hard” calcification (between caliper marks) in supraspinatus. The calcium has a convex superficial surface, casts an acoustic shadow, and elevates the bursal surface.

Tip:

Soft calcification responds well to aspiration, particularly if Doppler signal is present.

Several ultrasound-guided needle techniques have been advocated to treat rotator cuff calcification,[88],[89],[90],[91],[92] and the procedure is discussed in more detail in the interventional chapter (see Chapter 14).

I use a similar approach for both hard and soft calcifications. The patient is supine so as to avoid a vasovagal reaction. I use a 19G green needle to inject a mixture of long- and short-acting local anaesthetic and methylpredisolone into the bursa as described previously then advance the needle into the calcium. Hard calcium feels firm and may “crunch” when the needle enters. It does not usually yield an aspirate. I perform multiple needle perforations while trying to inject long-acting local anesthetic to disrupt the calcium. Soft calcium often spurts from the end of the needle when the syringe is detached. Even if it does, I try to aspirate as much calcium as possible by alternately injecting local anesthetic and aspirating. Sometimes the needle becomes blocked by calcium and has to be replaced. I do not inject steroid into the tendon. My experience is that this technique almost invariably relieves the pain of acute calcific tendonitis even if no aspirate is obtained. A similar technique also shows good short- and long-term results, although a proportion of patients suffer a recurrence of pain several weeks after the procedure and a minority requires a repeat procedure.[90]

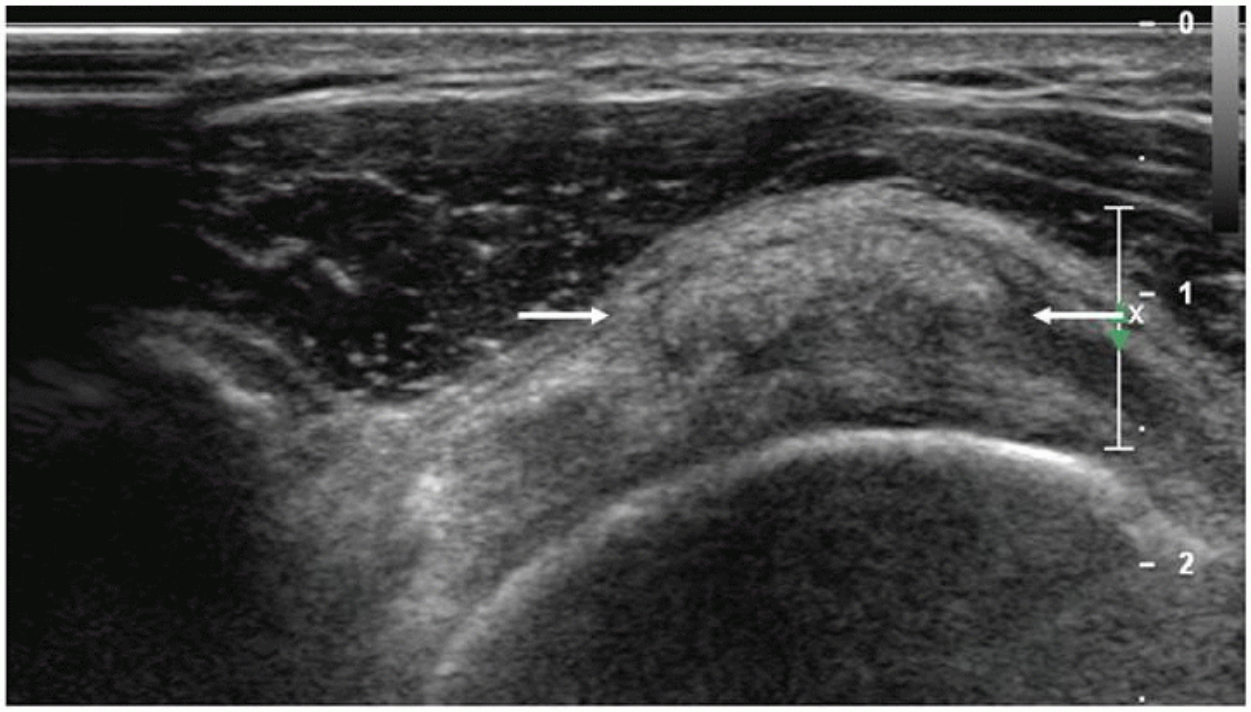

Figure 3.34. Large acute/soft calcific deposit (arrows) in subscapularis. The calcium is isoechoic to the tendon and elevates the bursal surface.

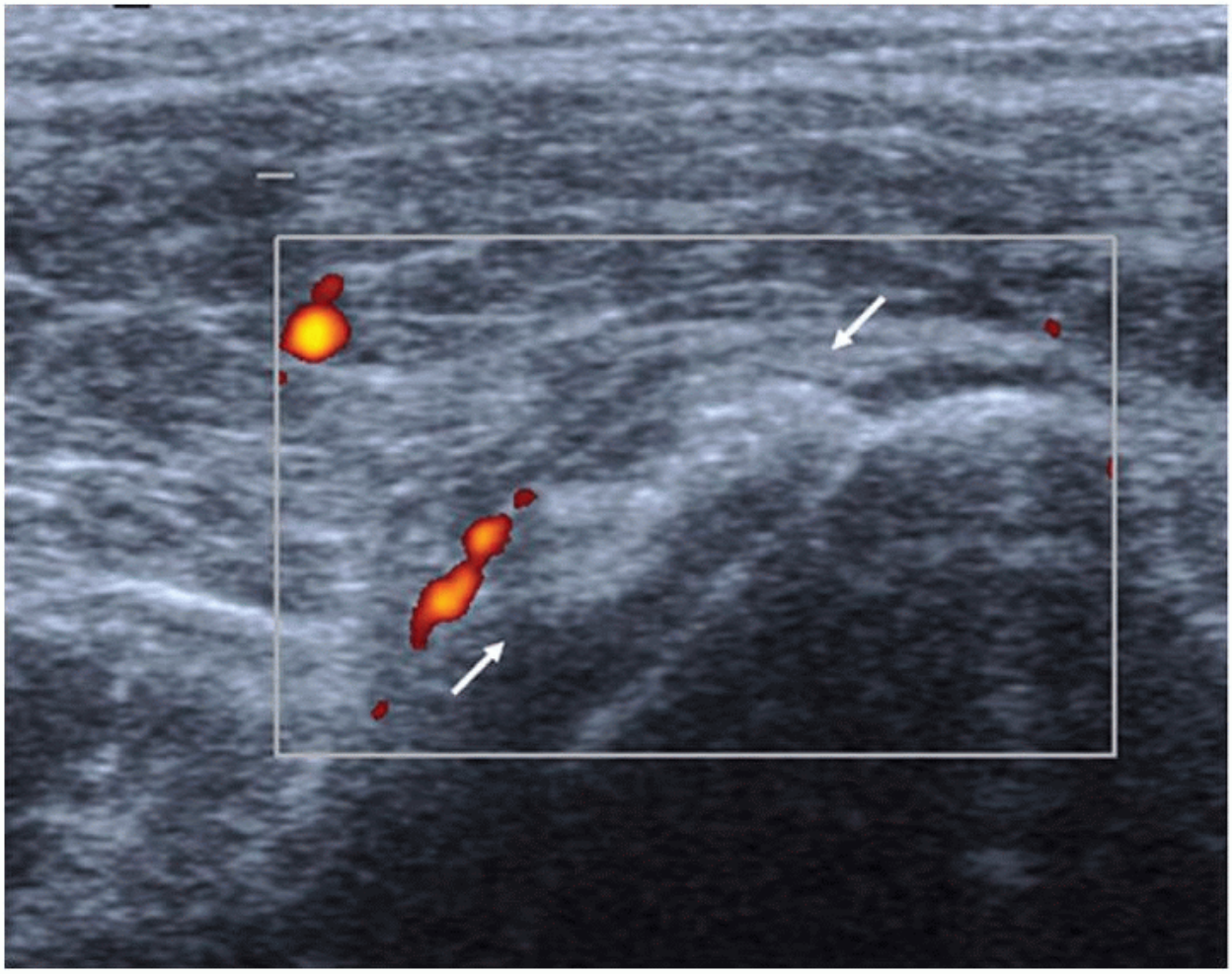

Figure 3.35. Large, acutely painful calcific deposit (arrows) in subscapularis. There is a small effusion in the bursa. Power Doppler shows neovascularity. Ultrasound-guided needle aspiration provides immediate and lasting pain relief.

Alternative techniques using needle sizes from 16G to 20G and one or two needles have been described.[89,90,91,92,93] The double needle technique flushes the calcium with saline using one needle to inject and the other to aspirate. Some authors advocate

injecting steroid into the bursa or the calcium or not injecting steroid. All report good results.[91,92,93,94,95]

Postoperative Shoulder

Assessment of the postoperative shoulder requires detailed information about the previous surgery. Recurrent tears are common and often asymptomatic, and there is frequently poor correlation between the clinical and imaging findings; but ultrasound assessment is accurate. Large tears, older patients, and multiple procedures are risk factors for recurrent tears.[93,94,95]

P. 41

Most surgeons use arthroscopy whenever possible rather than open arthrotomy. Subacromial decompression for impingement involves resection of the subdeltoid bursa and inferior acromion and release or resection of the CAL. Rotator cuff tears are treated by subacromial decompression and tendon repair. Partial-thickness tears may be debrided. Small full-thickness tears can be repaired by side-to-side sutures. Larger tears require the tendon to be reattached to bone, usually by bioabsorbable anchors placed in drill holes. Double row repair using distal and proximal anchors is said to promote healing and is currently popular. The distal anchors lie beyond the edge of the tendon.

Both the bursa and the CAL re-form after decompression and appear normal or thickened (Figs. 3.36 and 3.37). If the rotator cuff was intact at the time of surgery, the same criteria to diagnose a rotator cuff tear apply postoperatively as in a non-operated shoulder (Figs. 3.38 and 3.39).

A repaired tendon is often heterogeneously echogenic and has a flattened or depressed bursal surface. Thinning of the tendon is normal postoperatively. Anchors result in small defects in the humeral cortex. The tendon should be identified running to the defects (Fig. 3.40) or to a wider surgical trough in older repairs, but not to the distal anchor holes in double row repairs. If the tear is large and cannot be pulled fully back to the tuberosity, the anchor defects lie proximally, and the tuberosity is bare. Partial-thickness tears result in hypoechoic or mixed hypoechoic and hyperechoic defects on the articular side of the tendon.[93]

Tip:

Rotator cuff repair often results in heterogeneously increased echogenicity and bursal surface flattening.

Large recurrent tears that retract under the acromion result in non-visualisation of the tendon, usually with deltoid in direct contact with the humeral head and often with proximal migration of the humerus. Smaller tears result in discrete defects in the tendon. A gap between the tendon and the surgical defects in the humerus is convincing evidence of a tear. Occasionally in the immediate postoperative period, an anchor can be seen loose in the joint.[93,96,97]

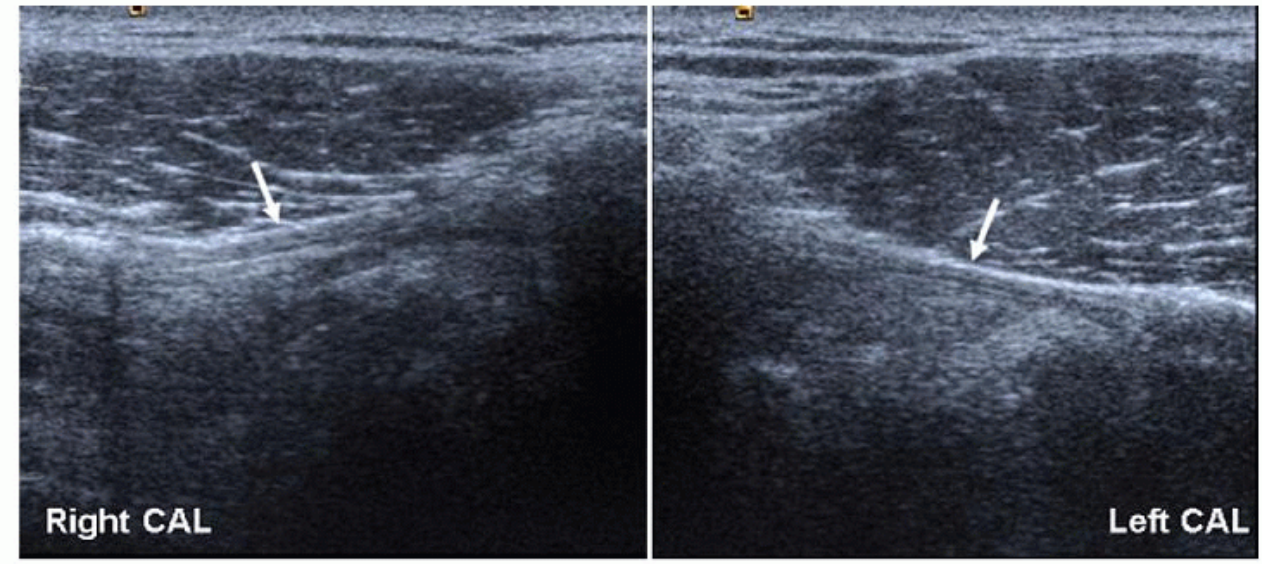

Figure 3.36. Previous subacromial decompression on right with release of the CAL. No surgery on left. The CALs appear identical.

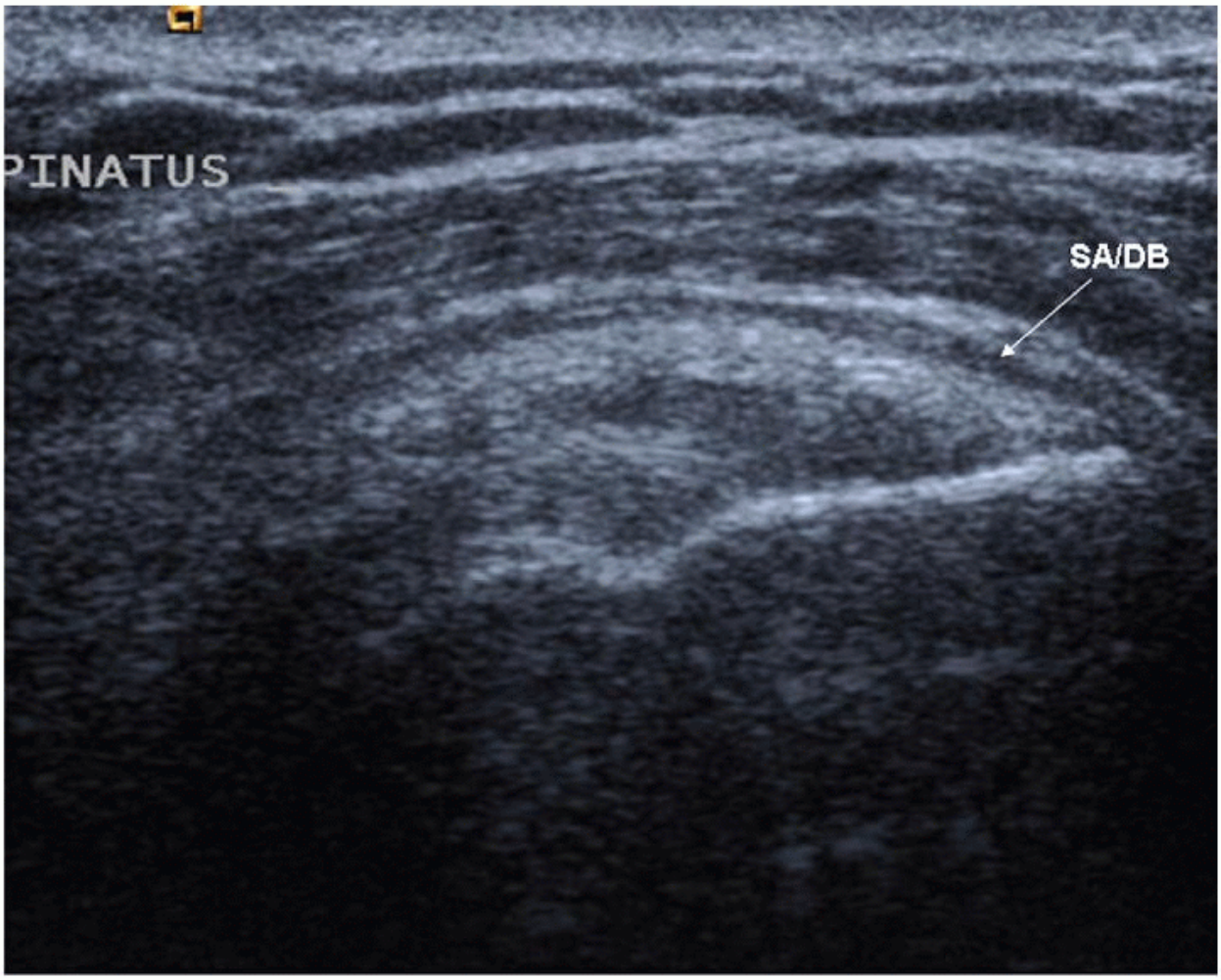

Figure 3.37. Subacromial decompression and excision of bursa 5 years previously. Good results but left with thickened bursa. SA/SB, subacromial/deltoid bursa.

Poor functional results following rotator cuff repair may be due to fatty atrophy of the muscles. Atrophy generally does not improve after cuff repair and may deteriorate. The same criteria apply as in the unoperated shoulder for the assessment of muscle atrophy.

Appearances vary after removal of calcium from the cuff. Complete resorption may be seen several years later. Other patients have residual streaks of calcium.

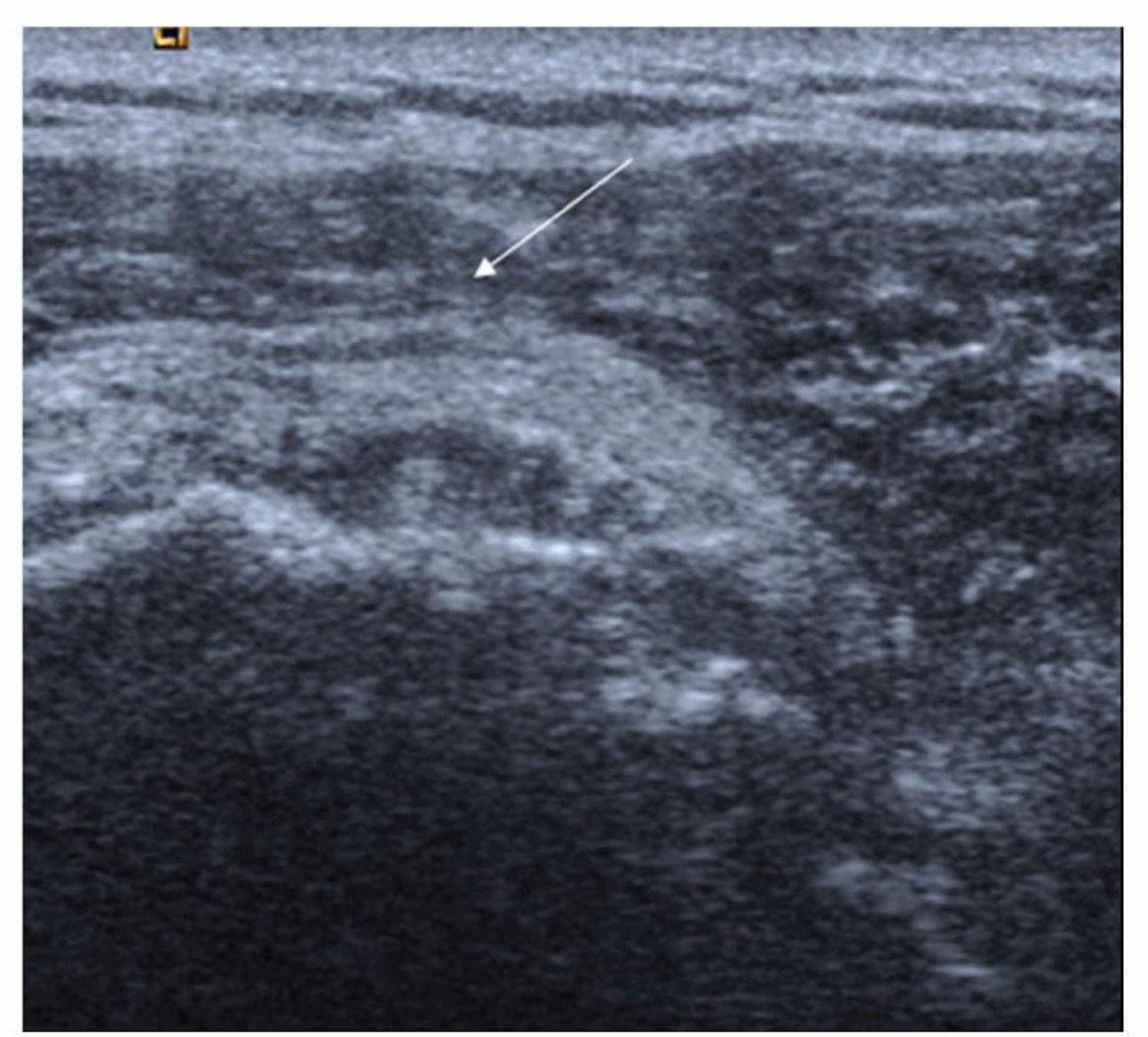

Figure 3.38. Previous subacromial decompression. Cuff intact at time of surgery. Now has thick bursa that is within normal limits, but there is bursal surface depression of supraspinatus, (arrow) indicating that there is a partial tear.
P. 42

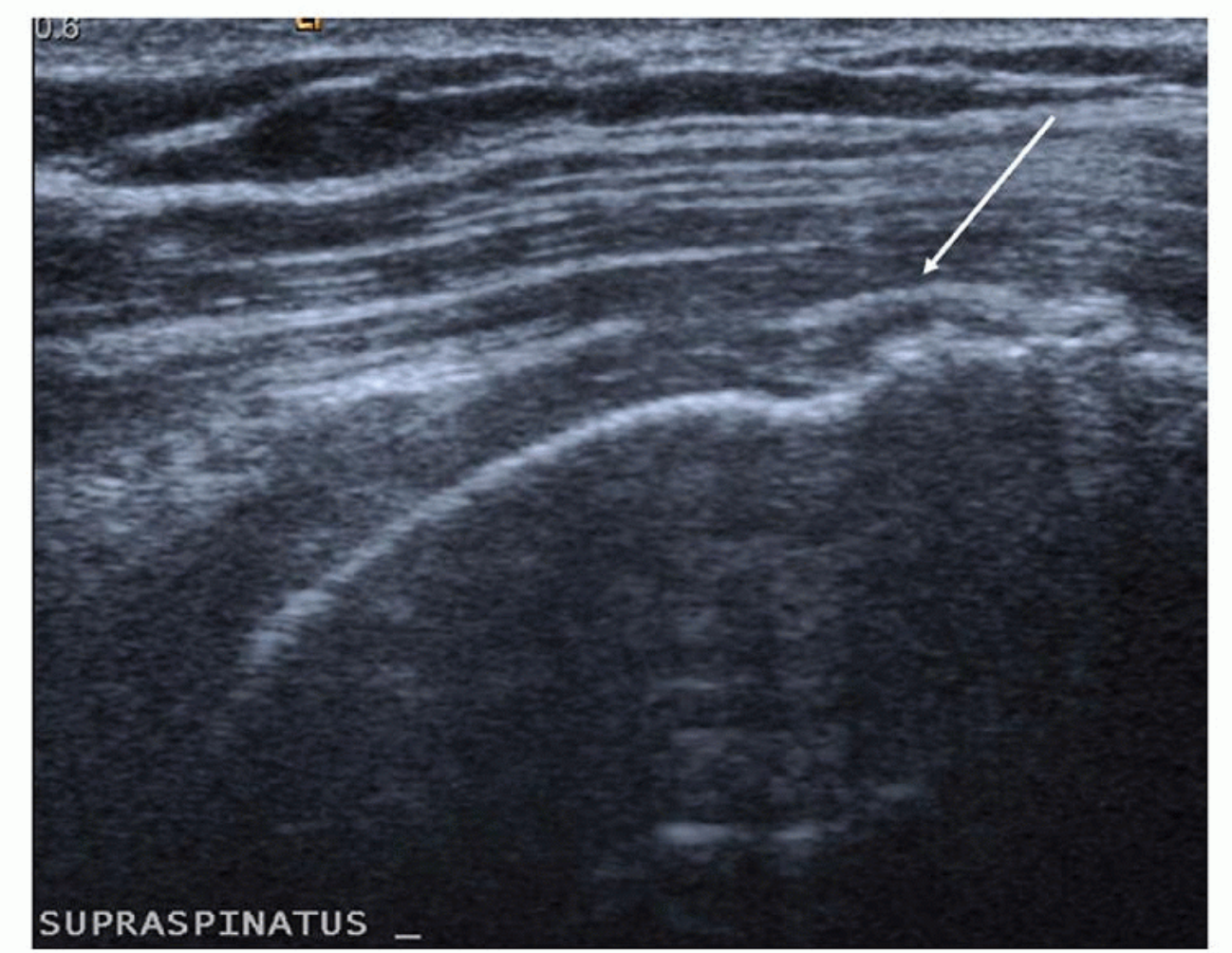

Figure 3.39. Previous decompression and debridement of partial thickness tear 7 years previously. Recent recurrence of pain. There is now a full-thickness tear, and the deltoid (arrow) is in direct contact with the humeral head.

Tenodesis of the LHB is performed for biceps tears and severe tendinosis. The tendon is detached from its origin at the superior rim of the glenoid and reattached to the humerus. If reattached proximally, the tendon may appear subluxed (Fig. 3.41) or dislocated from the bicipital groove. Distal reattachment results in an empty groove. Biceps tenotomy is sometimes performed in association with rotator cuff repairs in older or less active patients. The tendon is cut close to its origin and allowed to slip distally, resulting in an empty bicipital groove.

Conventional shoulder arthroplasty or hemiarthroplasty is performed for severe arthropathy when the rotator cuff is substantially intact; small tears can be repaired at the time of surgery. Reverse shoulder arthroplasty is performed in patients who have severe arthropathy and irreparable rotator cuff damage; the construction of the reverse prosthesis allows the deltoid to abduct the shoulder. The rotator cuff should be present following conventional arthroplasty, although postoperative tears are common. No cuff is visible after reverse arthroplasty.

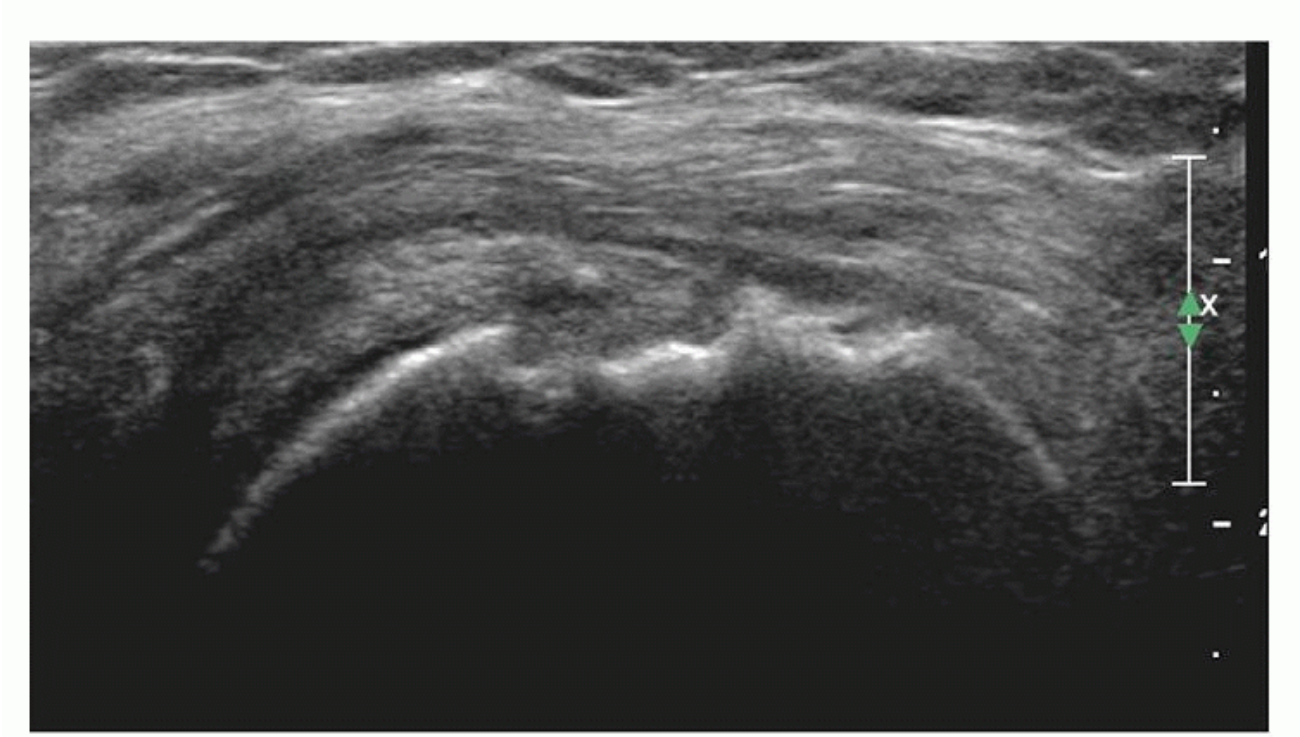

Figure 3.40. Intact supraspinatus following previous repair. The tendon runs into the surgical defect where it has been reattached.

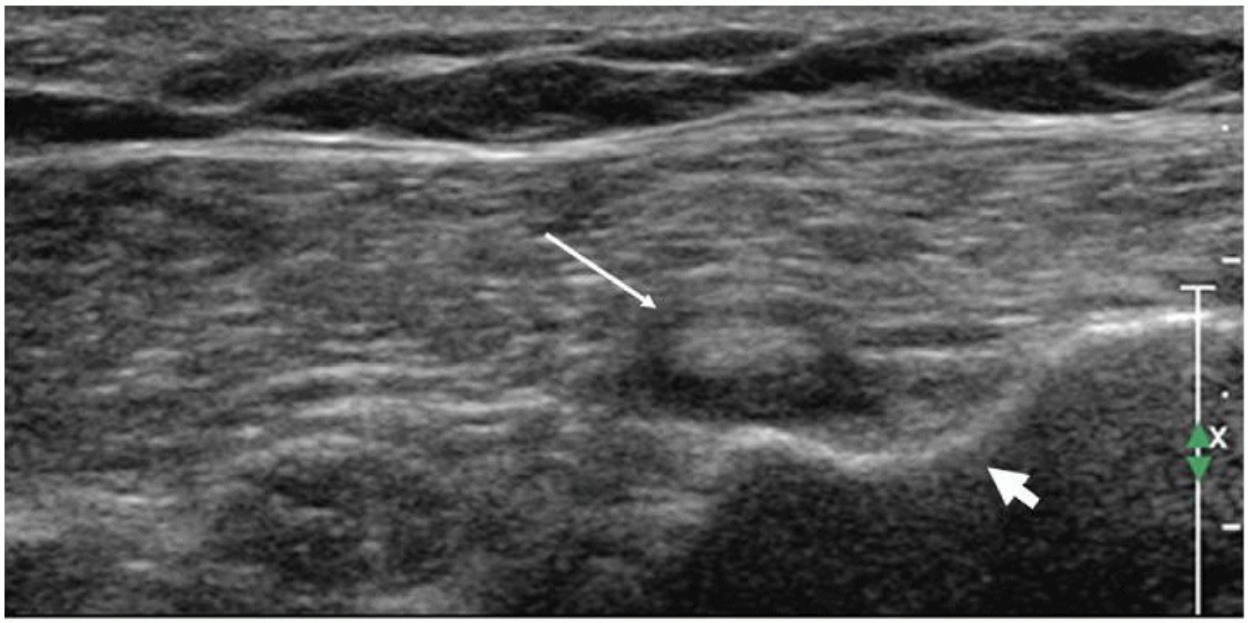

Figure 3.41. Following biceps tenodesis, the LHB tendon (long arrow) lies outside the bicipital groove (wide arrow).

Long head of Biceps Tendon

Biceps tendinopathy results from impingement against the coracoacromial arch and bicipital groove, and is often seen in patients with rotator cuff tears. Osteophytes and hyperostosis are frequently present at the entrance to the groove.[98]

Tendinopathy is best identified on transverse scans (Fig. 3.42A), which show an irregular contour, heterogeneous texture, and thickening or thinning of the tendon. Thinning occurs typically at the entrance to the bicipital groove, where osteophytes and hyperostosis may be identified. Longitudinal splits can be difficult to distinguish from congenitally bifid tendons, but other features of tendinopathy help, and the presence of a mesotendon for each moiety indicates a bifid tendon.

Fluid is frequently identified in the biceps tendon sheath. There is no definition of the difference between small normal, and large abnormal amounts of fluid, although it has been suggested that only a tiny amount of fluid posterior to the tendon is normal. A large effusion may be the result of intra-articular rather than biceps pathology, but it is always worth trying to identify tenosynovitis (Fig. 3.42B) using Doppler.[8]

Biceps instability (Fig. 3.43) results from rupture of its ligamentous stabilisers, particularly the CHL, either alone or in association with rupture of subscapularis. Biceps subluxes superficial to subscapularis if the ligaments are ruptured, and subscapularis is intact or only partly torn, and deep to subscapularis if the latter is completely torn.

The most obvious sign of a dislocated biceps is an empty groove. Biceps dislocation is distinguished from rupture by identifying the tendon lying medially, possibly as far medially as the coracoid process when subscapularis is ruptured and retracted. If biceps is not identified or cannot be distinguished from the short head of biceps tendon that arises from the coracoid process, it helps to place the transducer on the insertion of
P. 43

pectoralis major tendon on the humerus. This is at the level of the musculotendinous junction of the LHB, and it should be possible to follow the tendon proximally from there if it is present.[99,101]

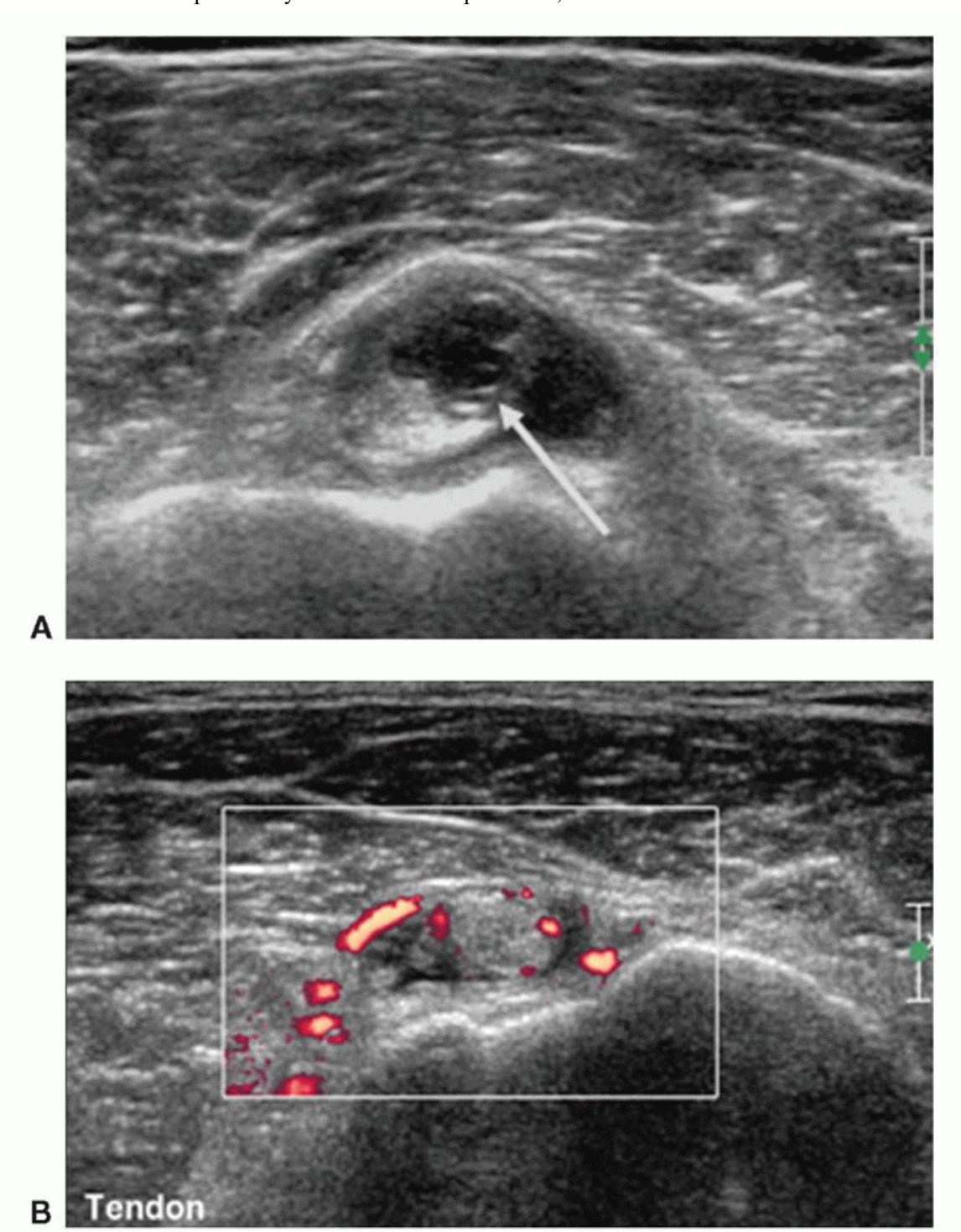

Figure 3.42. A: Short-axis scan of LHB, which is swollen and contains an intrasubstance tear (arrow). B: Power Doppler shows neovascularity in the LHB and its tendon sheath in keeping with tendinosis and associated tenosynovitis.

Tip:

If the biceps tendon is not visible, use transverse images to identify the pectoralis major insertion, which is at the level of the myotendinous junction of the biceps. Run the transducer proximally from the myotendinous junction to pick up the LHB tendon. Particularly when the subscapularis is intact, the subluxed biceps usually remains close to the groove or partly subluxed and lying at the edge of the groove. Intermittent subluxation can be demonstrated by dynamic examination with the elbow flexed at 90°. The

biceps slips medially out of the groove on external rotation and back in again on internal rotation.[101,102]
Tenodesis of biceps may move the tendon outside the bicipital groove, but it remains fixed in position during dynamic scanning.

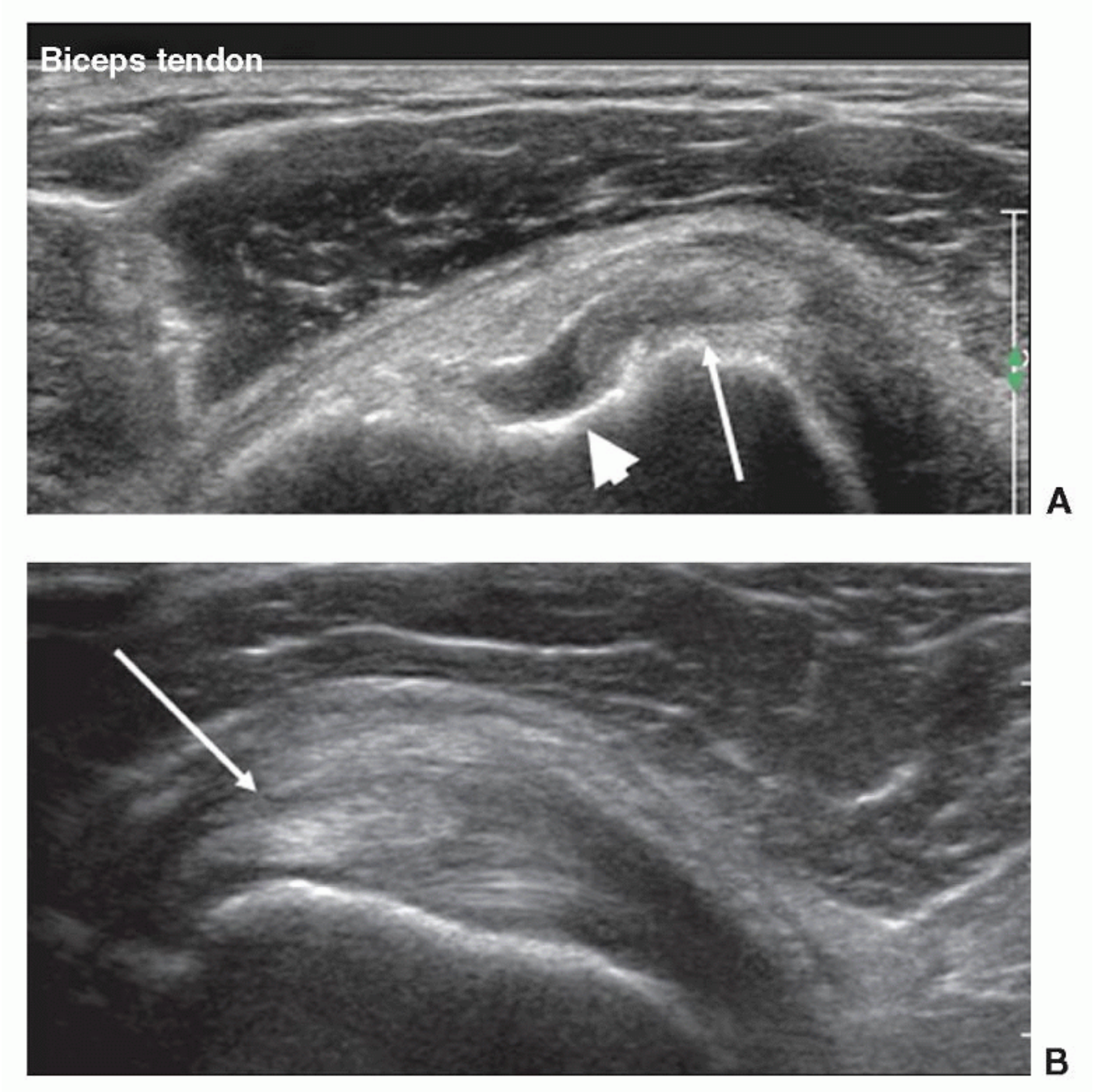

Figure 3.43. A: Transverse scan showing subluxed LHB (thin arrow) slipping out of bicipital groove (short arrow). B: Longitudinal scan showing subscapularis fibers superficial and deep to LHB (arrow), indicating a delaminating tear of subscapularis.
Complete rupture of the biceps tendon often occurs in association with large rotator cuff tears that extend across the rotator interval. Isolated tears are often clinically obvious as retraction of the muscle belly results in the “Popeye” sign. The fluid-filled tendon sheath lies in the bicipital groove and may contain debris or remnants of the tendon.
SLAP tears of the biceps origin cannot be identified on ultrasound. Magnetic resonance arthrography is the appropriate investigation for suspected SLAP tears.
Infection
Risk factors for infection include diabetes, renal failure, and immune suppression. Patients present with acute severe pain, pyrexia, and elevated inflammatory markers. The differential diagnosis is acute calcific tendonitis.
Fluid is the ultrasound hallmark of infection at the glenohumeral joint, subdeltoid bursa, or ACJ. The fluid may be thick and echogenic, but the ultrasound characteristics are nonspecific. Aspiration is essential if fluid is identified when infection is suspected. Ultrasound demonstrates even small-volume effusions that elevate the joint capsule at the posterior glenohumeral joint margin, best demonstrated with the hand across the chest (Fig. 3.17). This is a good site for aspiration. The biceps tendon sheath is the other reliable site to detect fluid.[103] In addition to distension with fluid, an infected bursa
P. 44

may be thick-walled and hyperaemic; and erosions may be present at an infected ACJ.[104,105]

Tip:

The posterior margin of the glenohumeral joint is the best place to identify and aspirate a joint effusion.

Instability

US may show a Hill-Sachs or reverse Hill-Sachs defect in the humeral head due to previous dislocation, damage to the glenoid or labrum or apparent joint laxity, but has no role in the assessment of glenohumeral instability.

Pectoralis Major

Injury to the pectoralis major is uncommon and due to forced extreme external rotation. Tears may involve muscle, musculotendinous junction, or tendon. Ultrasound shows a large hypoechoic haematoma, and muscle or tendon retraction.[106,107] The musculotendinous junction of the biceps is a good landmark for the pectoralis major insertion (Fig. 3.6).

Fractures

Ultrasound has no formal role in the assessment of fractures, but may show a depression in the posterolateral cortex of the humeral head due to the Hill-Sachs defect of anterior dislocation, or deep to subscapularis due to a reverse Hill-Sachs defect from posterior dislocation. Radiographically, occult tuberosity fractures can be associated with prolonged pain, restricted range of movement, and an intact but clinically weak supraspinatus following trauma. The cortex is undisplaced or minimally depressed or elevated, and the fracture line is seen as a tiny defect in the cortex. Overlying callus develops after several weeks.[102] With larger, displaced fragments, the tendon can usually be identified attached to the displaced bone.

Acromioclavicular Joint

Soft tissue hypertrophy and osteophytes occur with osteoarthritis (OA). Soft tissue swelling and erosions may be seen with rheumatoid arthritis (RA). Infection results in an effusion and possibly erosions.

Post-traumatic osteolysis of the clavicle results in irregular erosions at the outer end of the clavicle and widening, soft tissue swelling, and an effusion at the ACJ. Joint widening is also a feature of ACJ sprains. The “geyser sign” is a large cystic swelling filled with synovial fluid and extending superficially from the ACJ. It is due to direct communication between the glenohumeral joint and the ACJ through a large rotator cuff tear. Transducer pressure may demonstrate fluid moving through the ACJ, although not all ACJ cysts are associated with rotator cuff tears.[102,108]

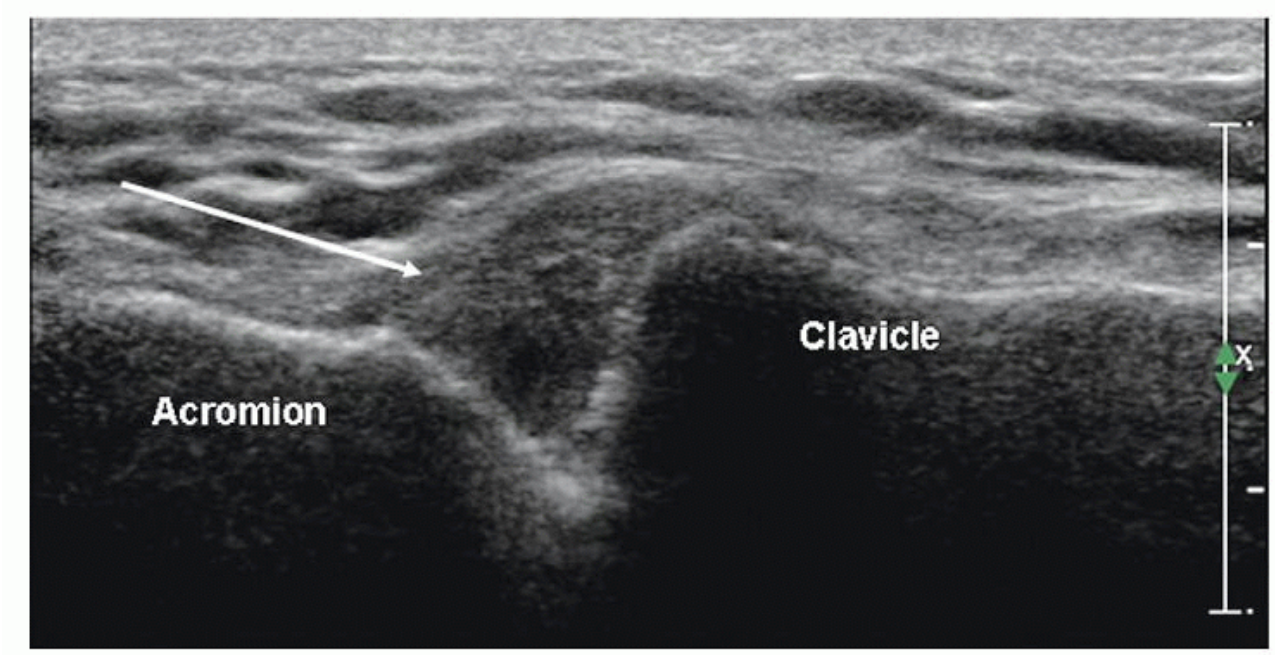

Figure 3.44. Long-axis scan of the ACJ (arrow).

Blind injection of the ACJ is difficult, particularly if there is much overlying soft tissue, because the joint is so narrow (Fig. 3.44). Ultrasound-guided injection is easy. The transducer is placed on the clavicle, oriented sagittally, and moved laterally to the acromion and back again. The bony structures are flat and densely echogenic. The ACJ is hypoechoic and disc-shaped (Fig. 3.45). After skin preparation, I use a green needle attached to a 5mL syringe. The needle is inserted into the joint either superior or inferior to the transducer. As the joint is often thick-walled, the needle position may have to be adjusted to ensure that the needle tip is in the joint space. This is confirmed by injecting a small volume of local anaesthetic. The ACJ has a small capacity and usually accepts <1 mL. If the injection is purely diagnostic (ie to see if it abolishes pain), I inject about 1mL of a mixture of lidocaine and bupivacaine. If steroid is to be injected for therapeutic benefit, the volume of anaesthetic injected should be just sufficient to show that the needle is intraarticular. I use methylprednisolone because it has a lower risk of causing skin depigmentation than triamcinolone. Most ACJ’s injected in this way will accept 20 to 30 mg of methylpredisolone. Pain relief as a result of the injection is a good prognostic test for surgical intervention but the effect of the steroid injection is usually short-lived.[109]

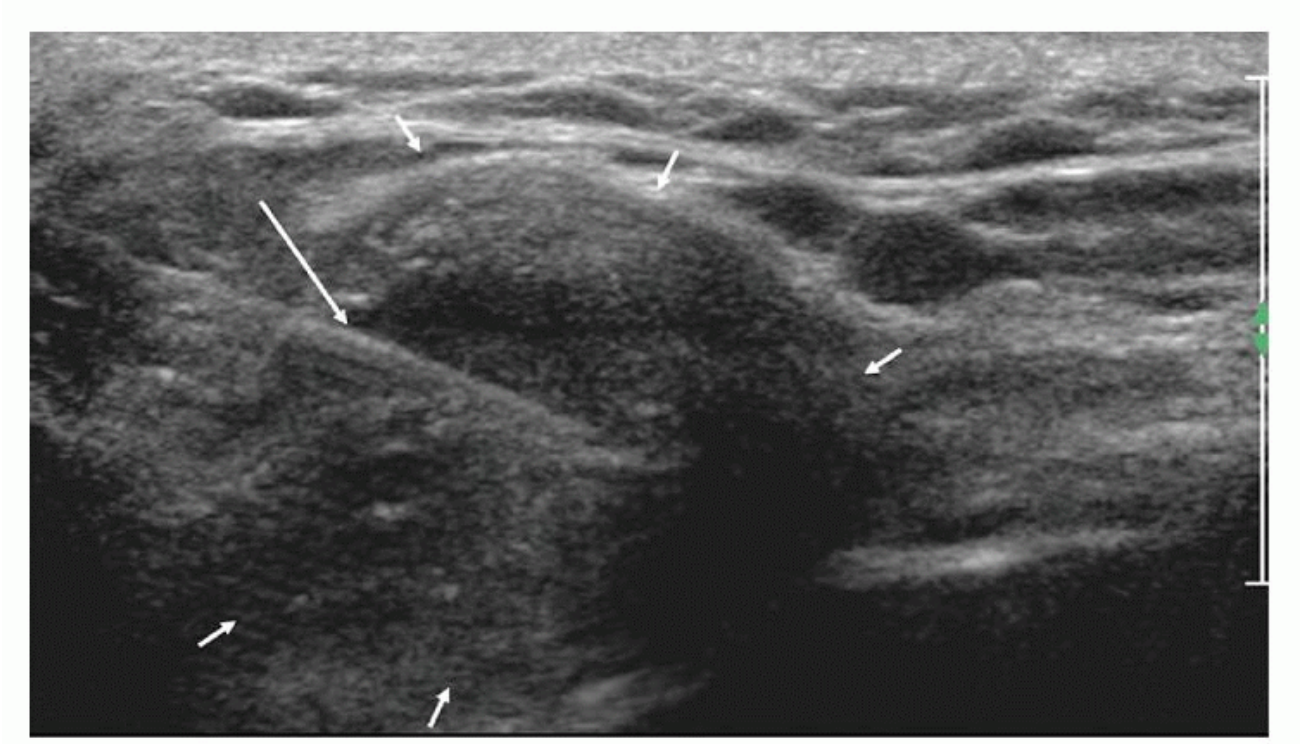

Figure 3.45. Sagittal scan showing needle insertion (long arrow) into hypoechoic, disc-like ACJ (short arrows).
P. 45

Masses

Lipomas are by far the most common tumours at the shoulder. If a mass cannot confidently be diagnosed as a lipoma or cyst on ultrasound, MRI and possibly biopsy will be needed.[110]

The other mass with a predilection for the shoulder region is elastofibroma dorsi, which almost always occurs deep to the inferior scapula. It is a pseudotumour composed of fat and fibroelastic tissue, probably due to friction between the scapula and chest wall, and is bilateral in about 50% of cases. The patient should be examined with the arm positioned to throw the scapula off the mass. Ultrasound shows multiple linear hypoechoic streaks against an echogenic background due to alternating tissue layers. Magnetic resonance imaging shows a poorly defined mass with alternating layers of fat and muscle signal intensity. The location, particularly if bilateral masses are present, and the ultrasound and MRI appearances, are characteristic. Biopsy and resection are unnecessary unless the lesion is symptomatic.[111],[112],[113]

Arthropathy: Osteoarthritis, Rheumatoid Arthritis, Crystal Deposition Disease, and Loose Bodies

Osteoarthritis causes osteophytes at the margins of the glenoid and humeral articular surfaces, joint space narrowing, and an effusion that may contain debris, loose bodies, and synovial hypertrophy.

Crystal deposition disease produces multiple small echogenic foci in cartilage, synovium, and joint fluid. Calcium pyrophosphate crystals are deposited within the hyaline cartilage, whereas monosodium urate crystals are deposited on the surface.[114],[115]

Rapidly progressive joint destruction associated with a massive rotator cuff tear and deposition of hydroxyapatite and pyrophosphate crystals occurs in “cuff tear arthropathy” or “Milwaukee shoulder.” The humerus is high-riding. Large and painful haemorrhagic joint effusions may contain debris, loose bodies, and hyperplastic synovium. Clinically, the effusion may simulate a large mass.[116]

Rheumatoid arthritis may affect the glenohumeral joint, ACJ, biceps tendon sheath, or, most frequently, the subdeltoid bursa. Ultrasound shows effusions, synovial proliferation, and hyperemia. It may be difficult to distinguish pannus from fluid even using sonopalpation. Early bone erosions may be present. Contrast-enhanced MRI is slightly superior to ultrasound in the detection of early inflammatory arthropathy at the shoulder.[117],[118] Ultrasound can locate the inflammation and be used to guide steroid injections.

Multiple small echogenic filling defects in the glenohumeral joint or subdeltoid bursa may be due to synovial chondromatosis or to rice bodies in association with RA or tuberculosis.[108]

CONCLUSION

Ultrasound is an important diagnostic tool in the management of many shoulder conditions. A good understanding of the anatomy and pathologic processes and meticulous technique are essential for good results. Ultrasound-guided interventions are widely employed, although their efficacy remains unproven.

REFERENCES

1. de Jesus JO, Parker L, Frangos AJ, et al. Accuracy of MRI, MR arthrography, and ultrasound in the diagnosis of rotator cuff tears: a meta-analysis. AJR Am J Roentgenol. 2009;92(6): 1701-1707.

2. Middleton WD, Payne WT, Teefey SA, et al. Sonography and MRI of the shoulder: comparison of patient satisfaction. AJR Am J Roentgenol. 2004;183(5):1449-1452.
3. Miller D, Frost A, Hall A. A 'one-stop clinic' for the diagnosis and management of rotator cuff pathology: getting the right diagnosis first time. Int J Clin Pract. 2008;62(5):750-753.
4. Beggs I, Bianchi S, Buero A, et al. Musculoskeletal ultrasound technical guidelines. I shoulder. http://essr.org/html/img/pool/shoulder.pdf.
5. Mochizuki T, Sugaya H, Uomizu M, et al. Humeral insertion of the supraspinatus and infraspinatus. New anatomical findings regarding the footprint of the rotator cuff. J Bone Joint Surg Am. 2008;90(5):962-969.
6. Soslowsky LJ, Carpenter JE, Bucchieri JS, et al. Biomechanics of the rotator cuff. Orthop Clin North Am. 1997;28(1):17-30.
7. Jamadar DA, Jacobson JA, Caoili EM, et al. Musculoskeletal sonography technique: focused versus comprehensive examination. AJR Am J Roentgenol. 2008;190(1):5-9.
8. Jacobson JA. Shoulder US: anatomy, technique, and scanning pitfalls. Radiology. 2011;260(1):6-16.
9. Krief OP. MRI of the rotator interval capsule. AJR Am J Roentgenol. 2005;184(5):1490-1494.
10. Petchprapa CN, Beltran LS, Jazrawi LM, et al. The rotator interval: a review of anatomy, function, and normal and abnormal MRI appearances. AJR Am J Roentgenol. 2010;195(3):567-576.
11. Adler RS, Fealy S, Rudzki JR, et al. Rotator cuff in asymptomatic volunteers: contrast-enhanced US depiction of intratendinous and peritendinous vascularity. Radiology. 2008;248(3):954-961.
12. Morag Y, Jacobson JA, Lucas D, et al. US appearance of the rotator cable with histologic correlation: preliminary results. Radiology. 2006;241(2):485-491.
13. Neer CS 2nd. Anterior acromioplasty for the chronic impingement syndrome in the shoulder: a preliminary report. J Bone Joint Surg Am. 1972;54(1):41-50.
14. Biberthaler P, Wiedemann E, Nerlich A, et al. Microcirculation associated with degenerative rotator cuff lesions. In vivo assessment with orthogonal polarization spectral imaging during arthroscopy of the shoulder. J Bone Joint Surg Am. 2003; 85-A(3):475-480.
15. Park HB, Yokota A, Gill HS, et al. Diagnostic accuracy of clinical tests for the different degrees of subacromial impingement syndrome. J Bone Joint Surg Am. 2005;87(7):1446-1455.
16. Kelly SM, Brittle N, Allen GM. The value of physical tests for subacromial impingement syndrome: a study of diagnostic accuracy. Clin Rehabil. 2010;24(2):149-158.
17. Beaudreuil J, Nizard R, Thomas T, et al. Contribution of clinical tests to the diagnosis of rotator cuff disease: a systematic literature review. Joint Bone Spine. 2009;76(1):15-19.
P. 46

18. Dinnes J, Loveman E, McIntyre L, et al. The effectiveness of diagnostic tests for the assessment of shoulder pain due to soft tissue disorders: a systematic review. Health Technol Assess. 2003;7(29):iii,1-166.
19. Kim HM, Dahiya N, Teefey SA, et al. Location and initiation of degenerative rotator cuff tears: an analysis of three hundred and sixty shoulders. J Bone Joint Surg Am. 2010;92(5):1088-1096.
20. Shindle MK, Chen CC, Robertson C, et al. Full-thickness supraspinatus tears are associated with more synovial inflammation and tissue degeneration than partial-thickness tears. J Shoulder Elbow Surg. 2011;20(6):917-927.
21. Hollister MS, Mack LA, Patten RM, et al. Association of sonographically detected subacromial/subdeltoid bursal effusion and intraarticular fluid with rotator cuff tear. AJR Am J Roentgenol. 1995;165(3):605-608.
22. Wohlwend JR, van Holsbeeck M, Craig J, et al. The association between irregular greater tuberosities and rotator cuff tears: a sonographic study. AJR Am J Roentgenol. 1998;171(1):229-233.
23. Arslan G, Apaydin A, Kabaalioglu A, et al. Sonographically detected subacromial/subdeltoid bursal effusion and biceps tendon sheath fluid: reliable signs of rotator cuff tear? J Clin Ultrasound. 1999;27(6):335-339.
24. Jacobson JA, Lancaster S, Prasad A, et al. Full-thickness and partial-thickness supraspinatus tendon tears: value of US signs in diagnosis. Radiology. 2004;230(1):234-242.
25. Fukuda H. The management of partial-thickness tears of the rotator cuff. J Bone Joint Surg Br. 2003;85(1):3-11.
26. Vinson EN, Helms CA, Higgins LD. Rim-rent tear of the rotator cuff: a common and easily overlooked partial tear. AJR Am J Roentgenol. 2007;189(4):943-946.
27. Bouffard JA, Lee SM, Dhanju J. Ultrasonography of the shoulder. Semin Ultrasound CT MR. 2000;21(3):164-191.
28. Crass JR, Craig EV, Feinberg SB. Clinical significance of sonographic findings in the abnormal but intact rotator cuff: a preliminary report. J Clin Ultrasound. 1988;16(9):625-634.
29. Farin PU, Jaroma H, Harju A, et al. Shoulder impingement syndrome: sonographic evaluation. Radiology. 1990;176(3):845-849.
30. Read JW, Perko M. Shoulder ultrasound: diagnostic accuracy for impingement syndrome, rotator cuff tear, and biceps tendon pathology. J Shoulder Elbow Surg. 1998;7(3):264-271.
31. Lewis JS, Raza SA, Pilcher J, et al. The prevalence of neovascularity in patients clinically diagnosed with rotator cuff tendinopathy. BMC Musculoskelet Disord. 2009;10:163.
32. Teefey SA, Rubin DA, Middleton WD, et al. Detection and quantification of rotator cuff tears. Comparison of ultrasonographic, magnetic resonance imaging, and arthroscopic findings in seventy-one consecutive cases. J Bone Joint Surg Am. 2004;86-A(4):708-716.
33. Fotiadou AN, Vlychou M, Papadopoulos P, et al. Ultrasonography of symptomatic rotator cuff tears compared with MR imaging and surgery. Eur J Radiol. 2008;68(1):174-179.

34. Al-Shawi A, Badge R, Bunker T. The detection of full-thickness rotator cuff tears using ultrasound. J Bone Joint Surg Br. 2008; 90(7):889-892.
35. Rutten MJ, Spaargaren GJ, van Loon T, et al. Detection of rotator cuff tears: the value of MRI following ultrasound. Eur Radiol. 2010;20(2):450-457.
36. Smith TO, Back T, Toms AP, et al. Diagnostic accuracy of ultrasound for rotator cuff tears in adults: a systematic review and meta-analysis. Clin Radiol. 2011;66(11):1036-1048.
37. Teefey SA, Middleton WD, Payne WT, et al. Detection and measurement of rotator cuff tears with sonography: analysis of diagnostic errors. AJR Am J Roentgenol. 2005;184(6):1768-1773.
38. Teefey SA, Hasan SA, Middleton WD, et al. Ultrasonography of the rotator cuff: A comparison of ultrasonographic and arthroscopic findings in one hundred consecutive cases. J Bone Joint Surg Am. 2000;82(4):498-504.
39. Kluger R, Mayrhofer R, Kröner A, et al. Sonographic versus magnetic resonance arthrographic evaluation of full-thickness rotator cufftears in millimeters. J Shoulder Elbow Surg. 2003;12(2): 110-116.
40. Strobel K, Zanetti M, Nagy L, et al. Suspected rotator cuff lesions: tissue harmonic imaging versus conventional US of the shoulder. Radiology. 2004;230(1):243-249.
41. Ferri M, Finlay K, Popowich T, et al. Sonography of fullthickness supraspinatus tears: comparison of patient positioning technique with surgical correlation. AJR Am J Roengenol. 2005;184(1):180-184.
42. Sasyniuk TM, Mohtadi NG, Hollinshead RM, et al. The interrater reliability of shoulder arthroscopy. Arthroscopy . 2007;23(9): 971-977.
43. Middleton WD, Teefey SA, Yamagichi K. Sonography of the rotator cuff: analysis of interobserver variability. AJR Am J Roentgenol. 2004;183(5):1465-1468.
44. O'Connor PJ, Rankine J, Gibbon WW, et al. Interobserver variation in sonography of the painful shoulder. J Clin Ultrasound. 2005;33(2):53-56.
45. Le Corroller T, Cohen M, Aswad R, et al. Sonography of the painful shoulder: role of the operator's experience. Skeletal Radiol. 2008;37(11):979-986.
46. Rutten MJ, Jager GJ, Kiemeney LA. Ultrasound detection of rotator cuff tears: observer agreement related to increasing experience. AJR Am J Roentgenol. 2010;195(6):W440-W446.
47. Moosmayer S, Heir S, Smith HJ. Sonography of the rotator cuff in painful shoulders performed without knowledge of clinical information: results from 58 sonographic examinations with surgical correlation. J Clin Ultrasound. 2007;35(1):20-26.
48. Hedtmann A, Fett H. Ultrasonography of the shoulder in subacromial syndromes with disorders and injuries of the rotator cuff [in German]. Orthopade. 1995;24(6):498-508.
49. Schibany N, Zehetgruber H, Kainberger F, et al. Rotator cuff tears in asymptomatic individuals: a clinical and ultrasonographic screening study. Eur J Radiol. 2004;51(3):263-268.
50. Worland RL, Lee D, Orozco CG, et al. Correlation of age, acromial morphology, and rotator cuff tear pathology diagnosed by ultrasound in asymptomatic patients. J South Orthop Assoc. 2003; 12(1):23-26.
51. Moosmayer S, Smith HJ, Tariq R, et al. Prevalence and characteristics of asymptomatic tears of the rotator cuff: an ultrasonographic and clinical study. J Bone Joint Surg Br. 2009;91(2):196-200.
52. Tempelhof S, Rupp S, Seil R. Age-related prevalence of rotator cuff tears in asymptomatic shoulders. J Shoulder Elbow Surg. 1999;8(4):296-299.
53. Kim HM, Teefey SA, Zelig A, et al. Shoulder strength in asymptomatic individuals with intact compared with torn rotator cuffs. J Bone Joint Surg Am. 2009;91(2):289-296.
54. Yamaguchi K, Tetro AM, Blam O, et al. Natural history of asymptomatic rotator cuff tears: a longitudinal analysis of asymptomatic tears detected sonographically. J Shoulder Elbow Surg. 2001;10(3):199-203.
55. Yamaguchi K, Ditsios K, Middleton WD, et al. The demographic and morphological features of rotator cuff disease. A comparison of asymptomatic and symptomatic shoulders. J Bone Joint Surg Am. 2006;88(8):1699-1704.
56. Wallny T, Wagner UA, Prange S, et al. Evaluation of chronic tears of the rotator cuff by ultrasound. A new index. J Bone Joint Surg Br. 1999;81(4):675-678.
57. Teefey SA, Middleton WD, Bauer GS, et al. Sonographic differences in the appearance of acute and chronic full-thickness rotator cuff tears. J Ultrasound Med. 2000;19(6):377-378.
58. Kim HM, Dahiya N, Teefey SA, et al. Relationship of tear size and location to fatty degeneration of the rotator cuff. J Bone Joint Surg Am. 2010;92(4):829-839.
59. Schaefer O, Winterer J, Lohrmann C, et al. Magnetic resonance imaging for supraspinatus muscle atrophy after cuff repair. Clin Orthop Relat Res. 2002;(403):93-99.
P. 47

60. Morag Y, Jacobson JA, Miller B, et al. MR imaging of rotator cuff injury: what the clinician needs to know. Radiographics. 2006;26(4):1045-1065.
61. Thomazeau H, Rolland Y, Lucas C, et al. Atrophy of the supraspinatus belly. Assessment by MRI in 55 patients with rotator cuff pathology. Acta Orthop Scand. 1996;67(3):264-268.
62. Khoury V, Cardinal E, Brassard P. Atrophy and fatty infiltration of the supraspinatus muscle: sonography versus MRI. AJR Am J Roentgenol. 2008;190(4):1105-1111.
63. Goutallier D, Postel JM, Lavau L, et al. Impact of fatty degeneration of the suparspinatus and infraspinatus muscles on the prognosis of surgical repair of the rotator cuff [in French]. Rev Chir Orthop Reparatrice Appar Mot. 1999;85(7):668-676.

64. Goutallier D, Postel JM, Bernageau J, et al. Fatty muscle degeneration in cuff ruptures. Pre- and postoperative evaluation by CT scan. Clin Orthop Relat Res. 1994;(304):78-83.
65. Goutallier D, Postel JM, Gleyze P, et al. Influence of cuff muscle fatty degeneration on anatomic and functional outcomes after simple suture of full-thickness tears. J Shoulder Elbow Surg. 2003;12(6):550-554.
66. Zanetti M, Gerber C, Hodler J. Quantitative assessment of the muscles of the rotator cuff with magnetic resonance imaging. Invest Radiol. 1998;33(3):163-170.
67. Mellado JM, Calmet J, Olona M, et al. Surgically repaired massive rotator cuff tears: MRI of tendon integrity, muscle fatty degeneration, and muscle atrophy correlated with intraoperative and clinical findings. AJR Am J Roentgenol. 2005;184(5):1456-1463.
68. Strobel K, Hodler J, Meyer DC, et al. Fatty atrophy of supraspinatus and infraspinatus muscles: accuracy of US. Radiology. 2005;237(2):584-589.
69. Kavanagh EC, Koulouris G, Parker L, et al. Does extended-field-of-view sonography improve interrater reliability for the detection of rotator cuff muscle atrophy? AJR Am J Roentgenol. 2008;190(1):27-31.
70. DeFranco MJ, Cole BJ. Current perspectives on rotator cuff anatomy. Arthroscopy. 2009;25(3):305-320.
71. Rutten MJ, Maresch BJ, Jager GJ, et al. Injection of the subacromial- subdeltoid bursa: blind or ultrasound-guided? Acta Orthop. 2007;78(2):254-257.
72. Henkus HE, Cobben LP, Coerkamp EG, et al. The accuracy of subacromial injections: a prospective randomized magnetic resonance imaging study. Arthroscopy. 2006;22(3):277-282.
73. Yamakado K. The targeting accuracy of subacromial injection to the shoulder: an arthrographic evaluation. Arthroscopy. 2002;18(8):887-891.
74. Kang MN, Rizio L, Prybicien M, et al. The accuracy of subacromial corticosteroid injections: a comparison of multiple methods. J Shoulder Elbow Surg. 2008;17(suppl 1):61-66.
75. Partington PF, Broome GH. Diagnostic injection around the shoulder: hit and miss? A cadaveric study of injection accuracy. J Shoulder Elbow Surg. 1998;7(2):147-150.
76. Ucuncu F, Capkin E, Karkucak M, et al. A comparison of the effectiveness of landmark-guided injections and ultrasonography guided injections for shoulder pain. Clin J Pain. 2009;25(9):786-789.
77. Naredo E, Cabero F, Beneyto P, et al. A randomized comparative study of short term response to injection versus sonographic-guided injection of local corticosteroids in patients with painful shoulder. J Rheumatol. 2004;31:308-314.
78. Ekeberg OM, Bautz-Holter E, Tveitå EK, et al. Subacromial ultrasound guided or systemic steroid injection for rotator cuff disease: randomised double blind study. BMJ. 2009;338:A3112.
79. Bureau NJ, Beauchamp M, Cardinal E, et al. Dynamic sonography evaluation of shoulder impingement syndrome. AJR Am J Roentgenol. 2006;187(1):216-220.
80. Bunker TD, Anthony PP. The pathology of frozen shoulder. A Dupuytren-like disease. J Bone Joint Surg Br. 1995;77:677-683.
81. Dias R, Cutts S, Massoud S. Frozen shoulder. BMJ. 2005; 331(7530):1453-1456.
82. Rodeo SA, Hannafin JA, Tom J, et al. Immunolocalization of cytokines and their receptors in adhesive capsulitis of the shoulder. J Orthop Res. 1997;15(3):427-436.
83. Lee JC, Sykes C, Saifuddin A, et al. Adhesive capsulitis: sonographic changes in the rotator cuff interval with arthroscopic correlation. Skeletal Radiol. 2005;34(9):522-527.
84. Homsi C, Bordalo-Rodrigues M, da Silva JJ, et al. Ultrasound in adhesive capsulitis of the shoulder: is assessment of the coracohumeral ligament a valuable diagnostic tool? Skeletal Radiol. 2006;35(9):673-678.
85. Mengiardi B, Pfirrrmann CW, Gerber C, et al. Frozen shoulder: MR arthrographic findings. Radiology. 2004;233(2):486-492.
86. Carette S, Moffet H, Tardif J, et al. Intraarticular corticosteroids, supervised physiotherapy, or a combination of the two in the treatment of adhesive capsulitis of the shoulder: a placebo- controlled trial. Arthritis Rheum. 2003;48(3):829-838.
87. Uhthoff HK, Loehr JW. Calcific tendinopathy of the rotator cuff: pathogenesis, diagnosis and management. J Am Acad Orthop Surg. 1997;5(4):183-191.
88. Farin PU, Jaroma H, Soimakallio S. Rotator cuff calcifications: treatment with US-guided technique. Radiology. 1995;195(3):841-843.
89. Aina R, Cardinal E, Bureau NJ, et al. Calcific shoulder tendinitis: treatment with modified US-guided fine-needle technique. Radiology. 2001;221(2):455-461.
90. del Cura JL, Torre I, Zabala R, et al. Sonographically guided percutaneous needle lavage in calcific tendinitis of the shoulder: short- and long-term results. AJR Am J Roentgenol. 2007;189(3):W128-W134.
91. Lin JT, Adler RS, Bracilovic A, et al. Clinical outcomes of ultrasound- guided aspiration and lavage in calcific tendinosis of the shoulder. HSS J. 2007;3(1):99-105.
92. Serafini G, Sconfienza LM, Lacelli F, et al. Rotator cuff calcific tendonitis: short-term and 10-year outcomes after twoneedle us-guided percutaneous treatment-nonrandomized controlled trial. Radiology. 2009;252(1):157-164.
93. Prickett WD, Teefey SA, Galatz LM, et al. Accuracy of ultrasound imaging of the rotator cuff in shoulders that are painful postoperatively. J Bone Joint Surg Am. 2003;85-A(6):1084-1089.
94. Galatz LM, Ball CM, Teefey SA, et al. The outcome and repair integrity of completely arthroscopically repaired large and massive rotator cuff tears. J Bone Joint Surg Am. 2004;86-A(2):219-224.
95. Gulotta LV, Nho SJ, Dodson CC, et al. Prospective evaluation of arthroscopic rotator cuff repairs at 5 years: part II-prognostic factors for clinical and radiographic outcomes. J Shoulder Elbow Surg. 2011;20(6):941-946.
96. Crass JR, Craig EV, Feinberg SB. Sonography of the postoperative rotator cuff. AJR Am J Roentgenol. 1986;146(3):561-564.

97. Mack LA, Nyberg DA, Matsen FR 3rd, et al. Sonography of the postoperative shoulder. AJR Am J Roentgenol. 1998;150(5):1089-1093.
98. Pfahler M, Branner S, Refior HJ. The role of the bicipital groove in tendinopathy of the long biceps tendon. J Shoulder Elbow Surg. 1999;8(5):419-424.
99. Bennett WF. Subscapularis, medial, and lateral head coracohumeral ligament insertion anatomy. Arthroscopic appearance and incidence of "'hidden" rotator interval lesions. Arthroscopy. 2001;17(2):173-180.
100. Patton WC, McCluskey GM 3rd. Biceps tendinitis and subluxation. Clin Sports Med. 2001;20(3):505-529.
101. Farin PU, Jaroma H, Harju A, et al. Medial displacement of the biceps brachii tendon: evaluation with dynamic sonography during maximal external shoulder rotation. Radiology. 1995;195(3):845-848.

102. Martinoli C, Bianchi S, Prato N, et al. US of the shoulder: nonrotator cuff disorders. Radiographics. 2003;23(2):381-401.
103. Zubler V, Mamisch-Saupe N, Pfirrmann CW, et al. Detection and quantification of glenohumeral joint effusion: reliability of ultrasound. Eur Radiol. 2011;21(9):1858-1864.
104. Cardinal E, Bureau NJ, Aubin B, et al. Role of ultrasound in musculoskeletal infections. Radiol Clin North Am. 2001;39(2):191-201.
105. Widman DS, Craig JG, van Holsbeeck M. Sonographic detection, evaluation, and aspiration of infected acromioclavicular joints. Skeletal Radiol. 2001;30(7):388-392.
106. Beloosesky Y, Grinblat J, Katz M, et al. Pectoralis major rupture in the elderly: clinical and sonographic findings. Clin Imaging. 2003;27(4):261-264.
107. Weaver JS, Jacobson JA, Jamadar DA, et al. Sonographic findings of pectoralis major tears with surgical, clinical, and magnetic resonance imaging correlation in 6 patients. J Ultrasound Med. 2005;24(1):25-31.
108. Mellado JM, Salvadó E, Camins A, et al. Fluid collections and juxta-articular cystic lesions of the shoulder: spectrum of MRI findings. Eur Radiol. 2002;12(3):650-659.
109. Bain GI, Van Riet RP, Gooi C, et al. The long-term efficacy of corticosteroid injection into the acromioclavicular joint using a dynamic fluoroscopic method. Int J Shoulder Surg. 2007;1:104-107.
110. Kransdorf MJ, Murphey MD. Soft tissue tumors in a large referral population: prevalence and distribution of diagnoses by age, sex and location. In: Imaging of Soft Tissue Tumors. Philadelphia, PA: WB Saunders,1997:3-35.
111. Naylor MF, Nascimento AG, Sherrick AD, et al. Elastofibroma dorsi: radiologic findings in 12 patients. AJR Am J Roentgenol. 1996;167(3):683-687.
112. Bianchi S, Martinoli C, Abdelwahab IF, et al. Elastofibroma dorsi: sonographic findings. AJR Am J Roentgenol. 1997;169(4):1113-1115.
113. Dalal A, Miller TT, Kenan S. Sonographic detection of elastofibroma dorsi. J Clin Ultrasound. 2003;31(7):375-378.
114. Ciapetti A, Filippucci E, Gutierrez M, et al. Calcium pyrophosphate dihydrate crystal deposition disease: sonographic findings. Clin Rheumatol. 2009;28(3):271-276.
115. Dalbeth N, McQueen FM. Use of imaging to evaluate gout and other crystal deposition disorders. Curr Opin Rhuematol. 2009;21(2):124-131.
116. Llauger J, Palmer J, Rosón N, et al. Nonseptic monoarthritis: imaging features with clinical and histopathologic correlation. RadioGraphics. 2000;20 Spec No:S263-S278.
117. Alasaarela E, Leppilahti J, Hakala M. Ultrasound and operative evaluation of arthritic shoulder joints. Ann Rheum Dis. 1998;57(6):357-360.
118. Hermann K-GA, Backhaus M, Schneider O, et al. Rheumatoid arthritis of the shoulder joint: comparison of conventional radiography, ultrasound, and dynamic contrastenhanced magnetic resonance imaging. Arthritis and Rheum. 2003;48(12):3338-3349.